

AD-A055 196

AIR FORCE INST OF TECH WRIGHT-PATTERSON AFB OHIO SCH--ETC F/G 1/3
THE TERRAIN FOLLOWING TASK FOR THE ADVANCED TACTICAL FIGHTER US--ETC(U)
DEC 77 R L SIMMONS
AFIT/6E/EE/77-39

UNCLASSIFIED

NL

1 OF 2

AD
A055196



①

THE TERRAIN FOLLOWING TASK
FOR THE ADVANCED TACTICAL FIGHTER
USING DISCRETE OPTIMAL CONTROL
THESIS

AFIT/GE/EE/77-39

Ross L. Simmons
Major USAF



Approved for public release; distribution unlimited.

78 06 13 168

6 THE TERRAIN FOLLOWING TASK
FOR THE ADVANCED TACTICAL FIGHTER
USING DISCRETE OPTIMAL CONTROL,

9 Master's Thesis,

Presented to the Faculty of the School of Engineering
of the Air Force Institute of Technology

Air University

in Partial Fulfillment of the
Requirements for the Degree of

Master of Science

12 I I P.

10 by
Ross E. Simmons, B.S.E.E.
Major USAF

Graduate Electrical Engineering

11 December 1977

ACCESSION for	
NTIS	White Section <input checked="" type="checkbox"/>
DDC	Buff Section <input type="checkbox"/>
UNANNOUNCED	<input type="checkbox"/>
JUSTIFICATION.....	
BY.....	
DISTRIBUTION/AVAILABILITY CODES	
Dist.	AVAIL. and/or SPECIAL
A	

Approved for public release; distribution unlimited.

012 225

slt

PREFACE

This study is an attempt to apply discrete optimal control theory to the design of a digital flight control system. I have chosen the terrain following task to illustrate the feasibility of such a control system. It would be helpful to the reader if he has a basic knowledge of optimal control theory and aircraft dynamics. I believe the development of the study is straight forward and could similarly be applied to any flight control task. I feel that digital control will bring about a minor revolution in the realm of aircraft performance. With the continued improvement in reliability and miniaturization of solid state devices, the flight control system of the future will be easily modified through software to perform a large variety of tasks. I further feel that discrete optimal control theory will form the foundation for the development of the required control laws. Optimal control has an intrinsic beauty that, unfortunately, I have only glimpsed.

I would like to express my deepest gratitude to my AFIT thesis advisor, Captain James E. Negro, for his encouragement and many helpful suggestions. I am also indebted to Michael J. Breza of the Aerospace Systems Division, Deputy for Development Planning, who sponsored this research effort. Finally, I wish to thank Major James E. Funk for his previous work which provided me with an optimal path for the terrain following mission.

Ross L. Simmons

Contents

	Page
Preface	ii
List of Figures	v
Abstract	viii
I. Introduction	1
Background	1
Digitization	2
Direct Digital Design	2
Scope	2
Assumptions	4
Thesis Organization	4
II. System Equations	6
Linearized Aircraft Model	7
Open Loop Dynamics Matrix, <u>A</u> , and Control	
Distribution Matrix, <u>B</u>	9
Output Matrix, <u>C</u>	11
III. Continuous Deterministic Regulator Problem	16
State Cost Matrix Development	17
Control Cost Matrix Development	21
Root-Locus	21
Closed Loop Pole Placement	22
Analog Computer Simulation	28
C* Time History	35
Summary	38
IV. Discrete Deterministic Regulator Problem	39
Discretization of the Continuous Plant	40
Discretization of a Continuous Performance	
Index	41
Discrete System Closed Loop Roots	42
Z-Plane Roots	43
Equivalent S-Plane Roots	45
Hybrid Regulator Simulation	46
Summary	48
V. The Terrain Following Task	55
Path Reconstruction	56
Reference Command Generator	57
Desired Velocity	58

Contents (Continued)

	Page
Reference Angle of Attack and Elevator Command	60
Reference Pitch Rate	67
Reference Thrust Command	67
Reference State and Control Vectors	68
Hybrid Simulation of the Terrain Terrain Following Task	69
VI. Conclusions and Recommendations	81
Conclusions	81
Recommendations for Further Study	82
Bibliography	83
Appendix A: Non-Linear Aircraft Model	85
Appendix B: REFCOM Program	89
Appendix C: Table of Discrete Feedback Gain Matrix Values	97
Vita	98

List of Figures

Figure .	Page
1 Reference command follower system for the terrain following task	3
2 Optimal Linear Regulator	6
3 State space block diagram for the regulator problem	7
4 Open loop dynamics matrix, <u>A</u> , and control distribution matrix, <u>B</u> , for .8 Mach at sea level	12
5 Output matrix, <u>C</u> , for .8 Mach at sea level	15
6 State cost matrix, <u>S</u>	20
7 Cornell Aeronautical Laboratory short period requirement "thumbprint"	22
8 Open loop eigenvalues and eigenvectors	23
9 Root-locus as a function of state cost q_3	25
10 Root-locus as a function of control cost r_1	25
11 Root-locus as a function of state cost q_1	26
12 Root-locus as a function of state cost q_4	26
13 Root-locus as a function of control cost r_2	27
14 Root-locus as a function of state cost q_2	27
15 Output cost matrix, state cost matrix, control cost matrix, and feedback gain matrix	29
16 Closed loop eigensystem	30
17 Aircraft open loop response to a one degree elevator command of one second duration	31
18 System closed loop response to an initial condition of 20 feet on the state variable h	32
19 System closed loop response to an initial condition of -20 feet per second on the state variable ' u '	33

List of Figures (Continued)

Figure	Page
20 System closed loop response to an initial condition of two degrees on the state variable θ	34
21 Normalized C^* response	37
22 Discrete closed loop root movement as a function of sample rate	43
23 Equivalent s-plane discrete closed loop root location as a function of sample rate	44
24 System closed loop response to an initial condition of 20 feet on the state variable h using a five hertz sample rate	49
25 System closed loop response to an initial condition of -20 feet per second on the state variable u using a five hertz sample rate	50
26 System closed loop response to an initial condition of two degrees on the state variable θ using a sample rate of five hertz	51
27 System closed loop response to an initial condition of 20 feet on the state variable h using a two hertz sample rate	52
28 System closed loop response to an initial condition of -20 feet per second on the state variable u using a two hertz sample rate	53
29 System closed loop response to an initial condition of two degrees on the state variable θ using a sample rate of two hertz.	54
30 Optimal cubic spline path and terrain for the hybrid simulation	70
31 Longitudinal velocity, u , as a function of time	73
32 Vertical velocity, w , as a function of time	73
33 Pitch rate, q , as a function of time	74
34 Pitch angle, θ , as a function of time	75

List of Figures (Continued)

Figure	Page
35 Elevator Angle, δ_e , as a function of time . . .	75
36 Thrust, T , as a function of time	76
37 Angle of attack, α , as a function of time . . .	76
38 Altitude, h , as a function of time	77
39 Error in altitude between actual and reference .	77
40 Error in longitudinal velocity between actual and reference	78
41 Error in vertical velocity between actual and reference	78
42 Error in pitch angle between actual and reference	79
43 Error in pitch rate between actual and reference	79
44 Error in thrust setting between actual and reference	80
45 Error in elevator deflection angle between actual and reference	80

Abstract

↓ Through the use of state space, continuous optimal control, and discrete optimal control, a digital flight control system was designed for the terrain following task. After formulating the aircraft linear perturbation model, the deterministic regulator problem was solved with a quadratic performance index to provide the desired continuous closed loop system. The system and performance index were then discretized to form a discrete deterministic regulator problem. This discrete regulator problem was then solved as a function of sample rate using eigenvector decomposition to determine a minimum acceptable rate for sampling. The effects of sample rate on the system were then examined. A sample rate of five hertz was shown to be high enough to adequately form the desired controls. A reference command generator based on constant energy path legs was developed to provide the required reference states and control inputs. The reference terrain following path was generated by an optimal cubic spline algorithm. The aircraft was shown to track the desired path in a highly acceptable manner through the use of a hybrid simulation. The design method utilized is recommended for consideration in designing the digital flight control system for other flight control tasks. ↑

THE TERRAIN FOLLOWING TASK
FOR THE ADVANCED TACTICAL FIGHTER
USING DISCRETE OPTIMAL CONTROL

I. Introduction

The breakthroughs of the past decade in the miniaturization and improved reliability of electronic devices have provided the control engineer with an alternate means of implementing an aircraft flight control system. Instead of the bellcranks, pushrods, and other mechanical linkages normally associated with an aircraft flight control system, it is now possible to use electrical signal paths for information transfer. The replacement provides a significant decrease in the weight and required size of the aircraft. This implementation has been accomplished in the F-16 aircraft by the use of an analog fly by wire flight control system. Further breakthroughs in the miniaturization and reliability of electronic devices have made the use of a digital computer instead of the analog computer highly feasible.

Background

The use of digital flight control techniques for aircraft control functions has been shown by recent research efforts using the A7-D and F-8 aircraft (Ref 1; Ref 2). There are many different design methods for digital controllers. These methods fall into two broad categories: (1) digitization, which is the discretization of a compensator designed in the continuous domain (s -plane), and (2) direct digital design, which is the direct design of the compensator in the

discrete domain (z- or w-plane).

Digitization. In a recent report by Honeywell (Ref 3), the digitization approach using the Tustin approximation is advocated. The Tustin transformation is a bilinear transformation technique that has the desirable properties of cascade preservation, stability invariance, and steady-state gain invariance. It is also relatively easy to apply and understand.

Another means of discretizing an s-plane compensator is the z-transformation. This method has the same properties as previously mentioned for the Tustin transformation except for cascade preservation. Of the numerous digitization techniques, the Tustin transformation and the z-transformation have found the widest use.

Direct Digital Design. As in the digitization process, there are several methods that can be applied to accomplish a direct digital design. These methods include, but are not limited to, pole-placement in the z-, w-, or w'-plane and a discrete design using optimal techniques. In a report by Powell, the discrete method was applied to the analysis of a digital system for a Boeing 737 aircraft with favorable results (Ref 4).

Scope

The scope of the problem addressed by this study is the design of the digital control laws for an advanced fighter aircraft performing the terrain following task. The aircraft is projected to be somewhat similar to the F-15. The design will be carried forth using the discrete optimal method es-

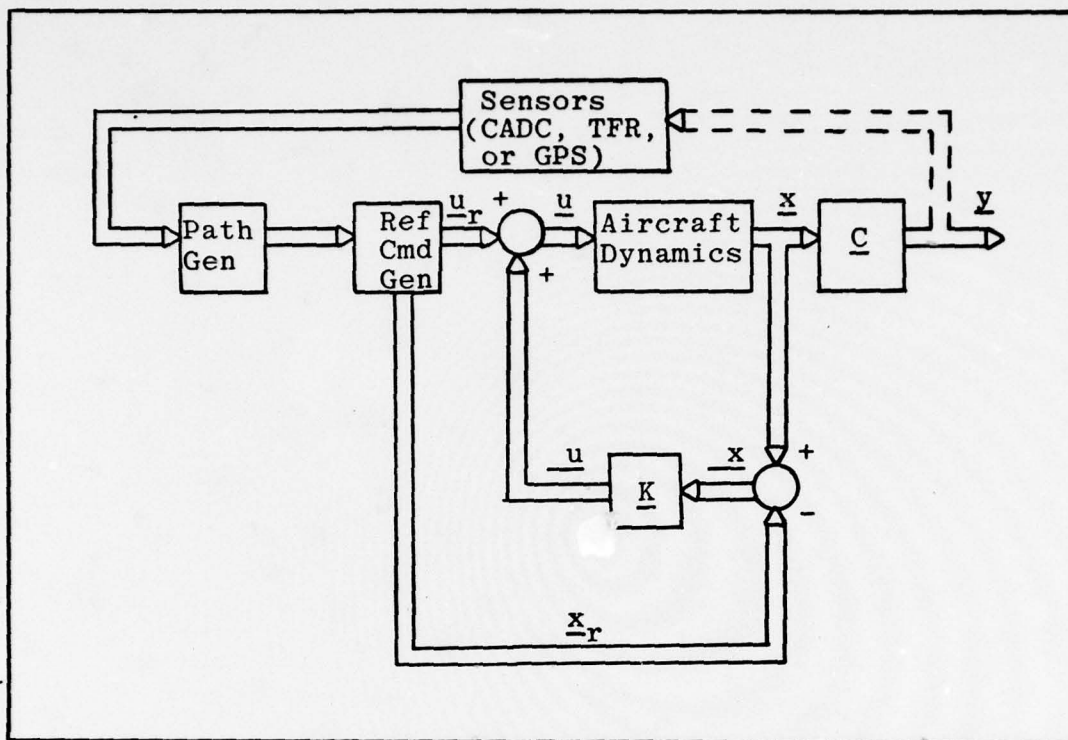


Figure 1. Reference command follower system for the terrain following task.

established by Katz and Powell (Ref 5). The design is based on reference control inputs to the elevator and thrust level and reference states provided by a reference command generator. The reference command generator receives its input from a path generator. The reference command follower system is shown in Figure 1. The reference states, \underline{x}_r , and reference commands, \underline{u}_r , are assumed to be available. One means of obtaining these values is shown in Chapter V.

The problem has been defined for the terrain following mode. This mode provides maneuvering in the vertical plane only; thus, the problem is limited to the longitudinal axis of the aircraft. The path tracking problem reduces to a reg-

ulator problem in the continuous domain. The state cost matrix, \underline{Q} , and the control cost matrix, \underline{R} , can then be determined for the quadratic performance index, J . With the cost values established, an evaluation of performance against C^* criteria is made, where C^* is defined as a blend of pitch-rate and normal acceleration (Ref 6). Using the cost values from the continuous system, the discrete optimal regulator problem is determined with sample rate as a parameter. The resulting system is then analyzed on a hybrid computer. The results are presented using s-plane, z-plane, and time response analyses of the system.

Assumptions

(1) The aircraft dynamics can be satisfactorily represented by the linearization of the aircraft motion about a nominal flight condition.

(2) The aircraft stability derivatives are valid for the flight regime investigated. In addition, these derivatives remain essentially the same along the reference flight trajectory as for the nominal flight condition.

(3) The optimal gain matrix is approximated as the steady-state solution to the Riccati equation.

(4) The reference states, \underline{x}_r , and reference commands, \underline{u}_r , are available.

Thesis Organization

Chapter II presents the system equations in the form of a linearized perturbation model. Chapter III illustrates the development of the system as a continuous regulator problem used in determining a satisfactory performance index. In

Chapter IV the discrete deterministic regulator problem is solved at various sample rates using the continuous performance index developed in Chapter III. An acceptable sample rate for use in the discrete system is, thus, obtained. A development of the necessary equations for use in the reference command generator is presented in Chapter V along with a hybrid simulation of the terrain following task. Chapter VI contains the conclusions and recommendations brought forth by this research effort.

II. System Equations

The reference command follower system, as shown previously in Figure 1, can be reduced to a regulator problem. This is done by setting the reference command, \underline{u}_r , and reference state, \underline{x}_r , equal to zero. The system then becomes the system as shown in Figure 2. Linearization of the aircraft equations of motion about the nominal flight condition provides a basis for the calculation of the feedback gain matrix, \underline{K} . The state space representation for this system is shown in Figure 3, where the open loop plant can be expressed as

$$\dot{\underline{x}} = \underline{A}\underline{x} + \underline{B}\underline{u} \quad (1)$$

$$\underline{y} = \underline{C}\underline{x} \quad (2)$$

For the purpose of this study it is required that:

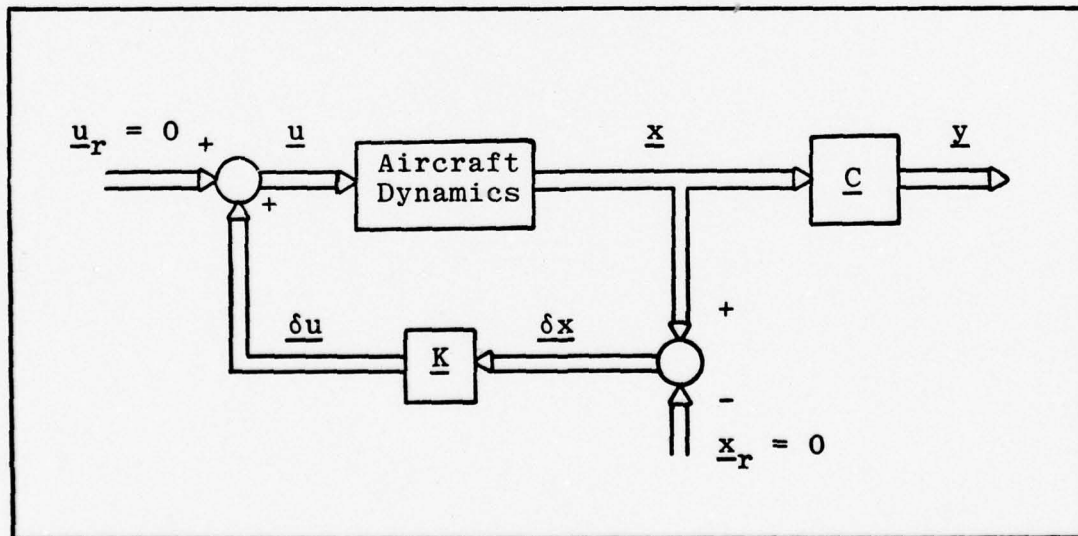


Figure 2. Optimal Linear Regulator.

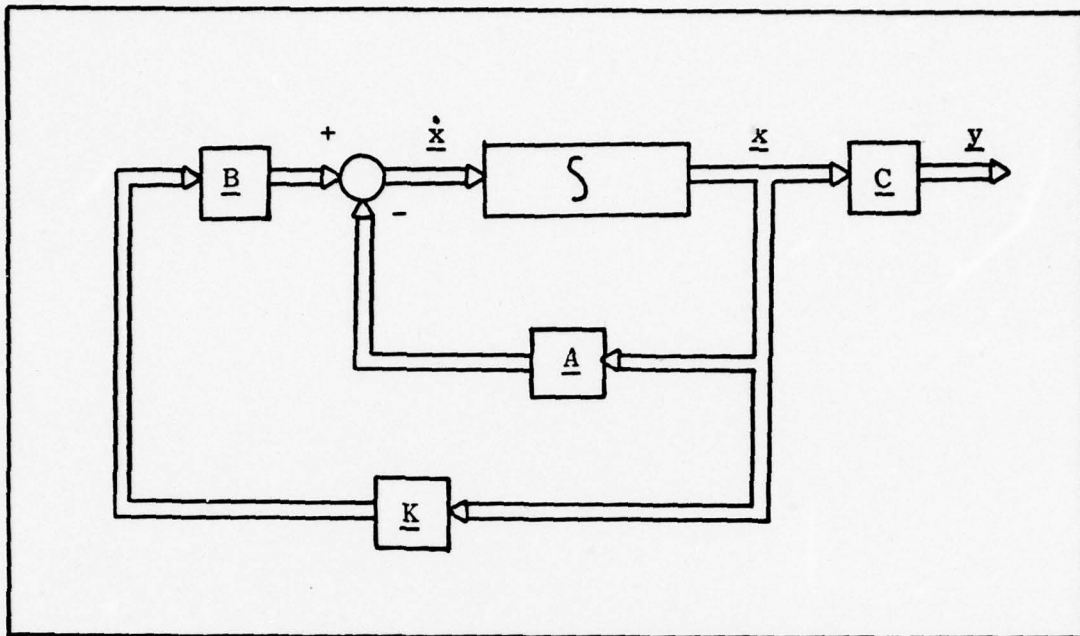


Figure 3. State space block diagram for the regulator problem.

1. All states are available for measurement.
2. The plant and control laws are linear.
3. The system is time invariant.

In addition the following techniques are used:

1. Only the infinite-time regulator is considered.
2. The performance index to be minimized is

$$J = \frac{1}{2} \int_0^{\infty} (\underline{y}^T \underline{Q} \underline{y} + \underline{u}^T \underline{R} \underline{u}) dt \quad (3)$$

with \underline{Q} symmetric non-negative definite and \underline{R} positive definite.

With these facts stated it is necessary to develop the required system equations.

Linearized Aircraft Model

The Assumed state variable vector is

$$\underline{x} = \begin{bmatrix} 'u & w & q & \theta & \delta e & \Delta T & h \end{bmatrix}^T \quad (4)$$

where

'u (ft/sec) is the perturbation in airspeed.

w (ft/sec) is the perturbation in vertical velocity.

q (rad/sec) is the perturbation in pitch rate.

θ (rad) is the perturbation in pitch angle.

δe (rad) is the perturbation in elevator deflection.

ΔT (lbs) is the perturbation in thrust.

h (ft) is the perturbation in distance from nominal flight path.

V_n (ft/sec) is the total forward nominal velocity.

Since it has been assumed the aerodynamic coefficients along the reference trajectory remain the same as for the nominal flight condition, then

$$\underline{\delta x} = \underline{x} - \cancel{\underline{x}_r}^0 \quad (5)$$

$$\underline{\delta \dot{x}} = \underline{A} \underline{x} + \underline{B} \underline{u} \quad (6)$$

where

$$\underline{\delta u} = \underline{u} - \cancel{\underline{u}_r}^0 \quad (7)$$

and

$$\underline{u} \equiv \begin{bmatrix} \delta e_c \\ \Delta T_c \end{bmatrix} \quad (8)$$

δe_c is the commanded elevator deflection in radians and ΔT_c is the commanded thrust change in pounds. Non-zero values for \underline{x}_r and \underline{u}_r are considered in Chapter V.

Open Loop Dynamics Matrix, A, and Control Distribution Matrix, B

In order to solve the regulator problem, it is first necessary to obtain the system equations in state space form using the dimensional stability derivatives. The longitudinal perturbation equations of motion can be represented by

$$\begin{aligned}\dot{u} &= X_u u + X_w w + X_q q - g \theta + X_{\delta e} \delta e + X_{\Delta T} \Delta T \\ \dot{w} &= Z_u u + Z_w w + (V_n + Z_q) q + Z_{\delta e} \delta e + Z_{\Delta T} \Delta T \\ \dot{q} &= M_u u + M_w w + M_q q + M_{\delta e} \delta e \\ \dot{\theta} &= q\end{aligned}\tag{9}$$

when the nominal pitch angle is zero (Ref 7: 4.113). The equation for the elevator servo can be approximated by the transfer function

$$\frac{\delta e(s)}{\delta e_c(s)} = \frac{1}{\tau_{\delta e} s + 1}\tag{10}$$

which can be written as

$$\dot{\delta e} = \frac{1}{\tau_{\delta e}} (\delta e_c - \delta e)\tag{11}$$

where $\tau_{\delta e}$ is the servo time constant and δe_c is the commanded change in elevator deflection. Similarly, for the throttle servo

$$\frac{\Delta T(s)}{\Delta T_c(s)} = \frac{1}{\tau_{\Delta T} s + 1}\tag{12}$$

which implies

$$\dot{\Delta T} = \frac{1}{\tau_{\Delta T}} (\Delta T_c - \Delta T) \quad (13)$$

where $\tau_{\Delta T}$ is the thrust servo time constant.

The relationship for \dot{h} is

$$\dot{h} = U \sin \theta - w \cos \theta \quad (14)$$

where $\theta = \theta_n + \theta$, i.e., nominal pitch attitude plus the perturbation in pitch. For the case under study, $\theta_n = 0$, thus

$$\dot{h} = U \sin \theta - w \cos \theta \quad (15)$$

When linearized, equation (15) becomes

$$\dot{h} = V_n \theta - w \quad (16)$$

Combining equations (9), (11), (13), and (16) into state space form yields

$$\dot{\underline{x}} = \underline{A} \underline{x} + \underline{B} \underline{u} \quad (1)$$

where the open loop dynamics matrix is

$$\underline{A} = \begin{bmatrix} X_u & X_w & X_q & -g & X_{\delta e} & X_{\Delta T} & 0 \\ Z_u & Z_w & (V_n - Z_u) & 0 & Z_{\delta e} & Z_{\Delta T} & 0 \\ M_u & M_w & M_q & 0 & M_e & 0 & 0 \\ 0 & 0 & 1 & 0 & 0 & 0 & 0 \\ 0 & 0 & 0 & 0 & -\frac{1}{\tau_{\delta e}} & 0 & 0 \\ 0 & 0 & 0 & 0 & 0 & -\frac{1}{\tau_{\Delta T}} & 0 \\ 0 & -1 & 0 & V_n & 0 & 0 & 0 \end{bmatrix} \quad (17)$$

and the control distribution matrix is

$$\underline{B} = \begin{bmatrix} 0 & 0 \\ 0 & 0 \\ 0 & 0 \\ 0 & 0 \\ \frac{1}{\tau_{\delta e}} & 0 \\ 0 & \frac{1}{\tau_{\Delta T}} \\ 0 & 0 \end{bmatrix} \quad (18)$$

Using the derivatives provided by the Avionics System Group, Aerospace Systems Division, Wright-Patterson Air Force Base, for a flight condition of .8 Mach (528kts or 882 ft/sec) at sea level, the open loop dynamics matrix and control distribution matrix become those shown in Figure 4.

Output Matrix, \underline{C}

The given outputs of the system are

$$\underline{y} = \underline{C} \underline{x} \quad (2)$$

which for the regulator problem becomes

$$\underline{y} = \underline{C} \underline{\delta x} \quad (19)$$

$$\text{since } \underline{\delta x} = \underline{x} \quad (5)$$

$$\text{and } \underline{\delta y} = \underline{y} \quad (7)$$

The specific outputs of the system are defined to be

$$\underline{y} \equiv \left[h \quad \frac{\dot{h}}{v_n} \quad \frac{\ddot{h}}{v_n^2} \quad 'u \right]^T \quad (20)$$

A =

-.7578E-02	.1276E-01	.3770E-01	-.3220E+02	-.3145E-03	.7130E-03	0.0
-.1029E+00	-.8198E+00	.8800E+03	0.0	-.4840E+02	-.3610E-04	0.0
-.1357E-03	-.6086E-02	-.2010E+00	0.0	-.4477E+01	0.0	0.0
0.0	0.0	.1000E+01	0.0	0.0	0.0	0.0
0.0	0.0	0.0	0.0	-.1000E+02	0.0	0.0
0.0	0.0	0.0	0.0	0.0	-.1000E+01	0.0
0.0	-.1000E+01	0.0	.8820E+03	0.0	0.0	0.0

B =

0.0	0.0
0.0	0.0
0.0	0.0
0.0	0.0
.1000E+02	0.0
0.0	.1000E+01
0.0	0.0

Figure 4. Open loop dynamics matrix, A, and control distribution matrix, B, for .8 Mach at sea level.

These outputs can be obtained from the aircraft navigation system and Central Air Data Computer (CADC). The variables used as outputs describe the aircraft flight path. The variable h is the deviation from the nominal altitude as previously defined. The remaining output variables are defined as

$$\frac{\dot{h}}{V_n} \approx \frac{dh}{dt} \cdot \frac{dt}{dR} = \frac{dh}{dR} = \gamma \quad (21)$$

where γ is the perturbation in flight path angle or slope of the flight path, and

$$\frac{\ddot{h}}{V_n^2} \approx \frac{d\gamma}{dR} = k \quad (22)$$

where k is the flight path curvature, and R is the horizontal range. It is preferable to work in range intervals, rather than time, for then the usual assumption of constant horizontal velocity is not required to relate the terrain locations to those of the aircraft (Ref 8). The variable u is the deviation from nominal airspeed as previously defined.

With these definitions in mind, it is now possible to determine the output matrix, \underline{C} . As shown in equation (16)

$$\dot{h} = -w + V_n \theta \quad (23)$$

If both sides of equation (23) are divided by V_n , the following relationship evolves

$$\gamma = \frac{h}{V_n} = -\frac{\dot{w}}{V_n} + \theta \quad (24)$$

Differentiating with respect to time and dividing by V_n yields

$$k = \frac{\ddot{h}}{V_n^2} = -\frac{\dot{\dot{w}}}{V_n^2} + \frac{q}{V_n} \quad (25)$$

When the value of \dot{w} from equation (9) is substituted into equation (25), equation (25) becomes

$$\begin{aligned} \frac{\ddot{h}}{V_n^2} &= \frac{-Z_u'u - Z_w\dot{w} - (\cancel{V_n} + Z_q q)q - Z_{\delta e}\delta e - Z_{\Delta T}\Delta T}{V_n^2} + \cancel{\frac{q}{V_n}} \\ &= \frac{-Z_u'u - Z_w\dot{w} - Z_q q - Z_{\delta e}\delta e - Z_{\Delta T}\Delta T}{V_n^2} \end{aligned} \quad (26)$$

Equations (24) and (26), along with h and $'u$ which are directly observable, can be combined to form the output matrix, \underline{C} .

$$\underline{C} = \begin{bmatrix} 0 & 0 & 0 & 0 & 0 & 0 & 1 \\ 0 & -\frac{1}{V_n} & 0 & 1 & 0 & 0 & 0 \\ \frac{-Z_u}{V_n^2} & \frac{-Z_w}{V_n^2} & \frac{-Z_q}{V_n^2} & 0 & \frac{-Z_{\delta e}}{V_n^2} & \frac{-Z_{\Delta T}}{V_n^2} & 0 \\ 1 & 0 & 0 & 0 & 0 & 0 & 0 \end{bmatrix} \quad (27)$$

With the system equations so defined, it is now possible to proceed with the solution of the regulator problem. The \underline{C} matrix for the aircraft at .8 Mach and at sea level is shown in Figure 5.

$\underline{C} =$

$$\begin{bmatrix} 0.0 & 0.0 & 0.0 & 0.0 & 0.0 & 0.0 & 0.0 & 0.0 & 0.0 & .1000E+01 \\ 0.0 & -.1134E-02 & 0.0 & .1000E+01 & 0.0 & 0.0 & 0.0 & 0.0 & 0.0 & 0.0 \\ .1323E-06 & .1054E-05 & .2571E-05 & 0.0 & .6222E-04 & .4641E-10 & 0.0 & 0.0 & 0.0 & 0.0 \\ .1000E+01 & 0.0 & 0.0 & 0.0 & 0.0 & 0.0 & 0.0 & 0.0 & 0.0 & 0.0 \end{bmatrix}$$

Figure 5. Output matrix, \underline{C} , for .8 Mach at sea level.

III. Continuous Deterministic Regulator Problem

The regulator problem involves a plant whose output, or any of the derivatives of the output, is initially nonzero. The objective is to provide a control to take the plant from this nonzero state to the zero state and to provide a satisfactory transient response. This is accomplished by providing a control composed of a linear combination of the states. Various methods have been presented in the literature for determining the necessary feedback gains for this control. For the problem under study, it is desired to minimize a quadratic performance index

$$J = \frac{1}{2} \int_0^{\infty} (\underline{x}^T \underline{S} \underline{x} + \underline{u}^T \underline{R} \underline{u}) dt \quad (28)$$

Bryson and Hall developed a computer program, OPTSYS, for the solution of this optimal control problem using eigenvector decomposition (Ref 9). This method was reported by them to be faster and more accurate for high order systems than the Ricatti equation method. Thus, the OPTSYS computer program is suited for use in determining the feedback gain matrix, \underline{K} . The control, \underline{u} , for the regulator becomes

$$\underline{u} = \underline{K} \underline{x} \quad (29)$$

where \underline{u} is composed of the change in elevator command, δe_c , and the change in commanded thrust level, ΔT_c . With the values for the feedback gain matrix available from OPTSYS, given a state cost matrix, \underline{S} , and a control cost matrix, \underline{R} , it is possible to obtain root-loci of the eigenvalues as a

function of the elements of \underline{S} and \underline{R} . From the root-loci and selective analog simulations, it becomes possible to determine a satisfactory state cost matrix and control cost matrix for use in the discrete optimal control problem.

State Cost Matrix Development

For the terrain following task, it is desired to minimize the energy of the output, \underline{y} , in conjunction with the control, \underline{u} , in the performance index

$$J = \frac{1}{2} \int_0^{\infty} (\underline{y}^T \underline{Q} \underline{y} + \underline{u}^T \underline{R} \underline{u}) dt \quad (3)$$

Thus, the output cost matrix of equation (3) must be related to the state cost matrix of equation (28) prior to use in the OPTSYS program. Since

$$\underline{y} = \underline{C} \underline{x} \quad (2)$$

$$\begin{aligned} \text{then } \underline{y}^T \underline{Q} \underline{y} &= (\underline{C} \underline{x})^T \underline{Q} (\underline{C} \underline{x}) \\ &= \underline{x}^T \underline{C}^T \underline{Q} \underline{C} \underline{x} \end{aligned} \quad (30)$$

and the state cost matrix becomes

$$\underline{S} = \underline{C}^T \underline{Q} \underline{C} \quad (31)$$

Since a diagonal cost matrix is often satisfactory, the output cost matrix is defined to be

$$\underline{Q} \equiv \begin{bmatrix} q_1 & 0 & 0 & 0 \\ 0 & q_2 & 0 & 0 \\ 0 & 0 & q_3 & 0 \\ 0 & 0 & 0 & q_4 \end{bmatrix} \quad (32)$$

Since there is an infinite number of possible choices for the q_i terms, a means of judiciously narrowing these choices must be used. One such method is to normalize the maximum RMS value of the output variables and their corresponding weighting factors to unity in defining the values for \underline{Q} . In the case at hand, the output variables are

$$\underline{y} = \begin{bmatrix} h & \frac{\dot{h}}{v_n} & \frac{\ddot{h}}{v_n^2} & 'u \end{bmatrix}^T \quad (20)$$

$$\text{thus } \underline{y}^T \underline{Q} \underline{y} = h^2 q_1 + \left(\frac{\dot{h}}{v_n} \right)^2 q_2 + \left(\frac{\ddot{h}}{v_n^2} \right)^2 q_3 + 'u^2 q_4 \quad (33)$$

If the maximum value for each term is set equal to one, the q_i terms can be defined as

$$q_1 \equiv \frac{1}{(h_m)^2} \quad (34)$$

$$q_2 \equiv \frac{1}{(\dot{h}_m/v_n)^2} \quad (35)$$

$$q_3 \equiv \frac{1}{(\ddot{h}_m/v_n^2)^2} \quad (36)$$

$$q_4 \equiv \frac{1}{(\dot{u}_m)^2} \quad (37)$$

where the subscript m denotes the variables maximum value. It can be observed from the foregoing that equal weight has been placed on the maximum RMS value of each output variable. While this weighting may not produce a desirable system, it does have the benefit of intuitive appeal and does yield a starting point for the iterative design approach. The next step is to select what is felt to be the maximum allowable values for the output variables.

The maximum deviation from commanded flight path, h_m , is chosen as 20 feet. The maximum rate of change in the deviation from flight path, \dot{h}_m , is chosen to be 40 feet per second. For the acceleration term, \ddot{h}_m , a value of 40 feet per second squared is chosen. The initial value for the maximum deviation in airspeed, u_m , is 100 feet per second. These maximum values may be rather large, but provide a realistic starting point for forming the root-loci of the system.

Using the values presented above, the output cost matrix becomes

$$Q = \begin{bmatrix} 0.0025 & 0.0 & 0.0 & 0.0 \\ 0.0 & 486.2 & 0.0 & 0.0 \\ 0.0 & 0.0 & 3.78E08 & 0.0 \\ 0.0 & 0.0 & 0.0 & 0.0001 \end{bmatrix} \quad (38)$$

The state cost matrix is derived from the relationship shown

$\underline{S} =$

1.066E-04	5.269E-05	1.285E-04	0.0	3.111E-03	2.320E-09	0.0
5.269E-05	1.045E-03	1.024E-03	-5.512E-01	2.478E-02	1.840E-08	0.0
1.285E-04	1.024E-03	2.498E-03	0.0	6.046E-02	4.510E-08	0.0
0.0	-5.512E-01	0.0	4.862E+02	0.0	0.0	0.0
3.111E-03	2.478E-02	6.046E-02	0.0	1.463E+00	1.091E-06	0.0
2.320E-09	1.849E-08	4.510E-08	0.0	1.091E-06	8.140E-13	0.0
0.0	0.0	0.0	0.0	0.0	0.0	2.500E-03

Figure 6. State cost matrix, \underline{S} , for $q_1 = .0025$, $q_2 = 486.2$, $q_3 = 3.78E08$, $q_4 = .0001$.

in equation (31). For the values of \underline{Q} in equation (38), the state cost matrix is shown in Figure 6.

Control Cost Matrix Development

The control cost matrix, \underline{R} , is initially established in the same manner as that for the output cost matrix. Namely,

$$\underline{R} = \begin{bmatrix} r_1 & 0 \\ 0 & r_2 \end{bmatrix} \quad (39)$$

where r_1 is the weight on the control energy of δe_c and r_2 is the weight on the throttle (thrust) control, ΔT_c . Thus,

$$r_1 = \frac{1}{(\delta e_{c_m})^2 (\text{Rad})^2} = \frac{(57.3)}{(\delta e_{c_m})^2 (\text{deg})^2} \quad (40)$$

$$r_2 = \frac{1}{(\Delta T_{c_m})^2} \quad (41)$$

With the methods established for determining the state and control cost matrices, it is now possible to proceed with a root-locus study of the system.

Root-Locus

The root-loci for the system are determined by varying the cost functions which results in a variation in the state feedback gain quantities and, thus a change in the location of the characteristic roots. In the following figures depicting the root-loci, a single cost parameter is varied while the other parameters are held constant. The associated regulator problem for each variation in cost is then solved to yield the closed loop eigenvalues (roots) and feedback gains

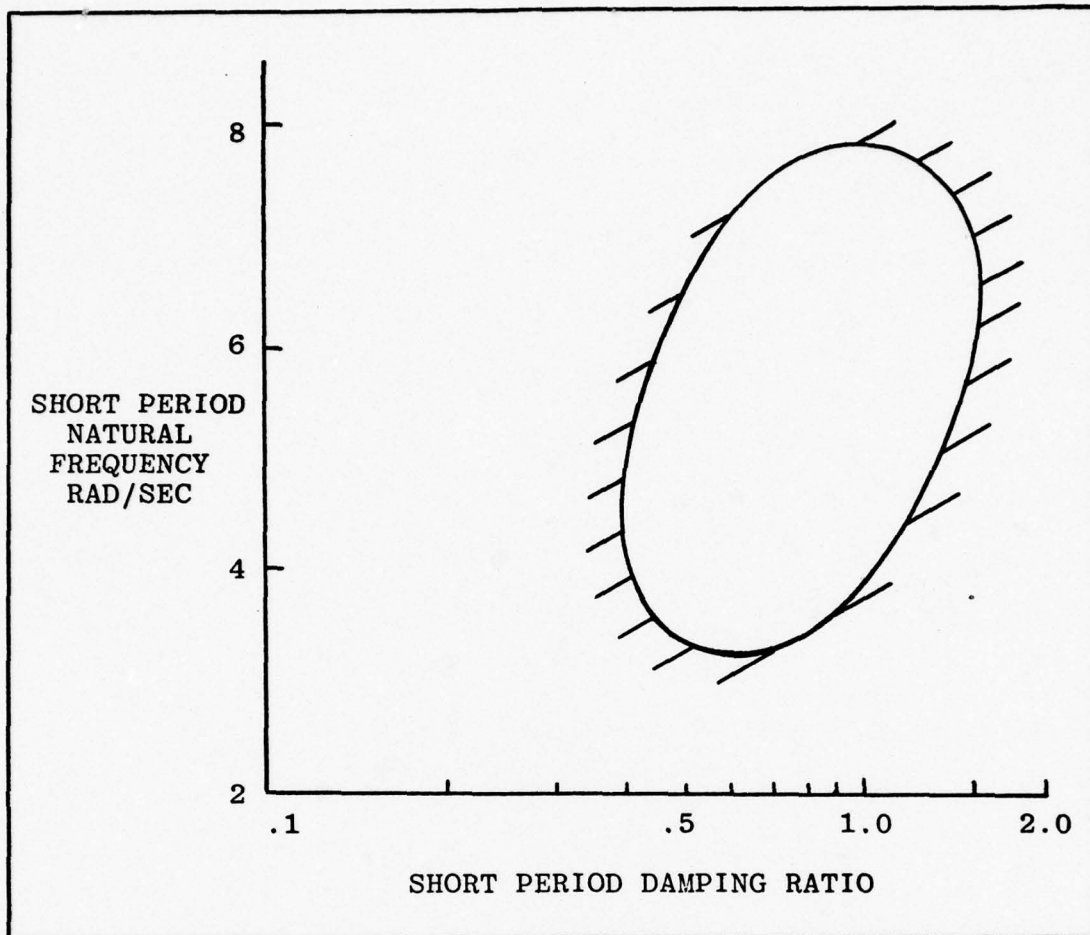


Figure 7. Cornell Aeronautical Laboratory short period requirement "thumbprint".

using the OPTSYS program. The root locations are then plotted as a function of the cost parameter.

Closed Loop Pole Placement

With the root-loci as design tools, the closed loop roots can be placed at a desired operating point by a judicious choice of the state and control cost parameters. Using the Cornell Aeronautical Laboratory "thumbprint" shown in Figure 7 as a guide, a damping ratio of approximately .7 and a natural frequency of five radians per second was chosen as the desired

OPEN LOOP

EIGENVALUES	EIGENVECTORS
$-.511 \pm j 2.293$	$.715E-02 \pm j .761E-02$ 1.000 $.352E-03 \pm j .261E-02$ $.105E-02 \pm j .387E-03$ 0.0 0.0 $-.135 \pm j .622E-01$
$-.328E-02 \pm j .547E-01$	$-.362E-01 \pm j .463E-02$ $.914E-03 \pm j .145E-03$ $-.339E-05 \pm j .350E-06$ $-.268E-05 \pm j .622E-04$ 0.0 0.0 1.000
0.0	0.0 0.0 0.0 0.0 0.0 0.0 1.000
-10.000	$-.262E-02$ $-.9995$ $.119E-01$ $-.119E-02$ $.275E-01$ 0.0 $.533E-02$
-1.000	$-.717E-03$ $.101E-04$ $-.449E-07$ $.448E-07$ 0.0 1.000 $-.295E-04$

Figure 8. Open loop eigenvalues and eigenvectors.

operating point for the short period roots. The open loop eigensystem is depicted in Figure 8. The root-loci are shown in Figures 9 through 14.

As shown in Figure 9, if the cost parameter q_3 is set equal to $6.72\text{E}+10$, \ddot{h}_m equal to three feet per second squared, the desired root location has been approximated. This root location is $-3.8 \pm j 3.44$ with a damping ratio of .74 and a natural frequency of 5.1 radians per second. As indicated in Figure 10, the control cost parameter r_1 could also be used either independently or in conjunction with q_3 to achieve the desired pole placement. The problem encountered in using the control cost parameter is that to achieve the desired pole placement would require additional control energy. It is felt at this point that the one and one-half degree elevator deflection, as it relates to energy, is sufficient.

Figure 11 shows the root-locus as a function of state cost parameter q_1 , the weight on the h term of the output. A decrease in the q_1 term can be thought of in direct correlation to how fast the regulator drives an initial condition on the state h toward zero. Initially, the phugoid root will be placed at $-.273 \pm j .268$ which has a damping ratio of .71 and a natural frequency of .38 radians per second. This corresponds to q_1 equal to $2.5\text{E}-03$ which is based on h_m equal to twenty feet as derived previously in this chapter.

The remaining roots of interest are the roots that correspond to the airspeed and thrust response. As shown in Figures 12 and 13, these root locations can be varied using

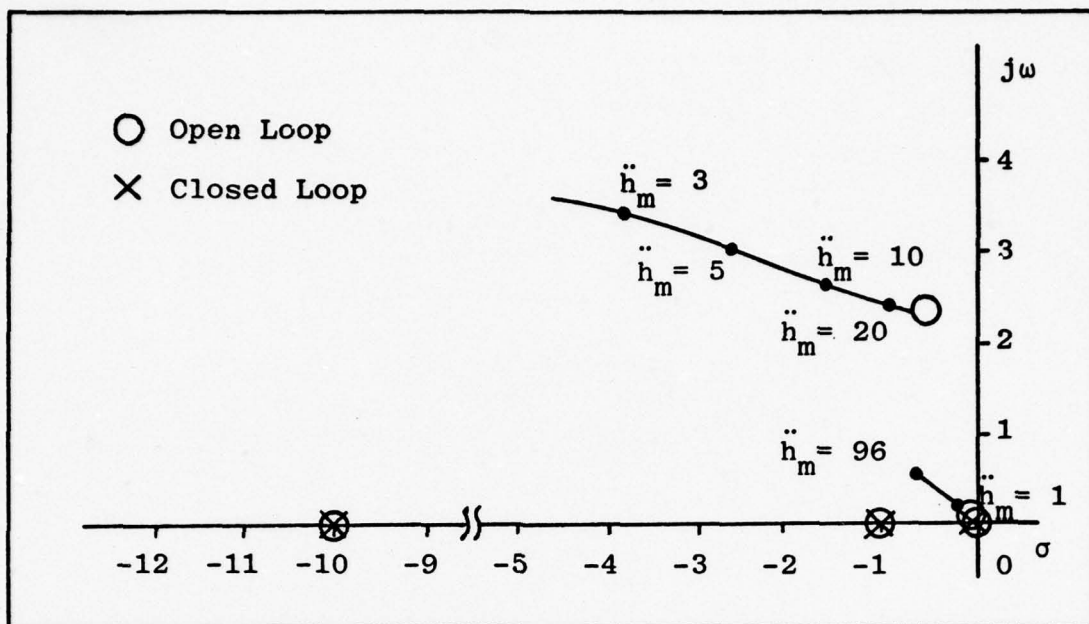


Figure 9. Root-locus as a function of state cost q_3 with $q_1 = .0025$, $q_2 = 486.2$, $q_4 = .0001$, $r_1 = 1459$, $r_2 = 6.25E-08$.

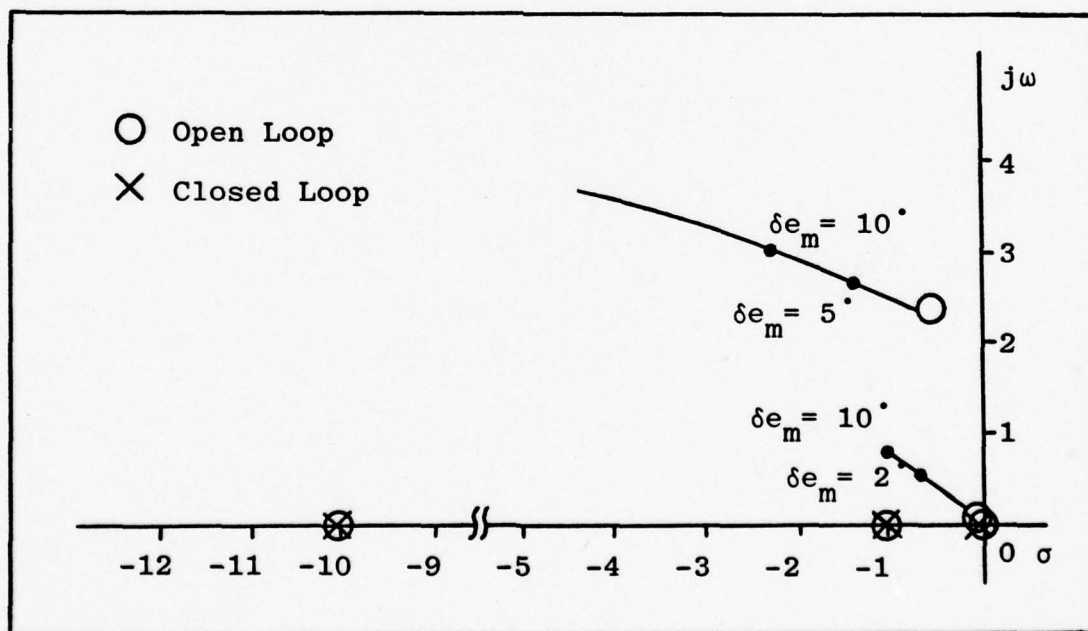


Figure 10. Root-locus as a function of control cost r_1 with $q_1 = .0025$, $q_2 = 486.2$, $q_3 = 3.78E+08$, $q_4 = .0001$, $r_2 = 6.25E-08$.

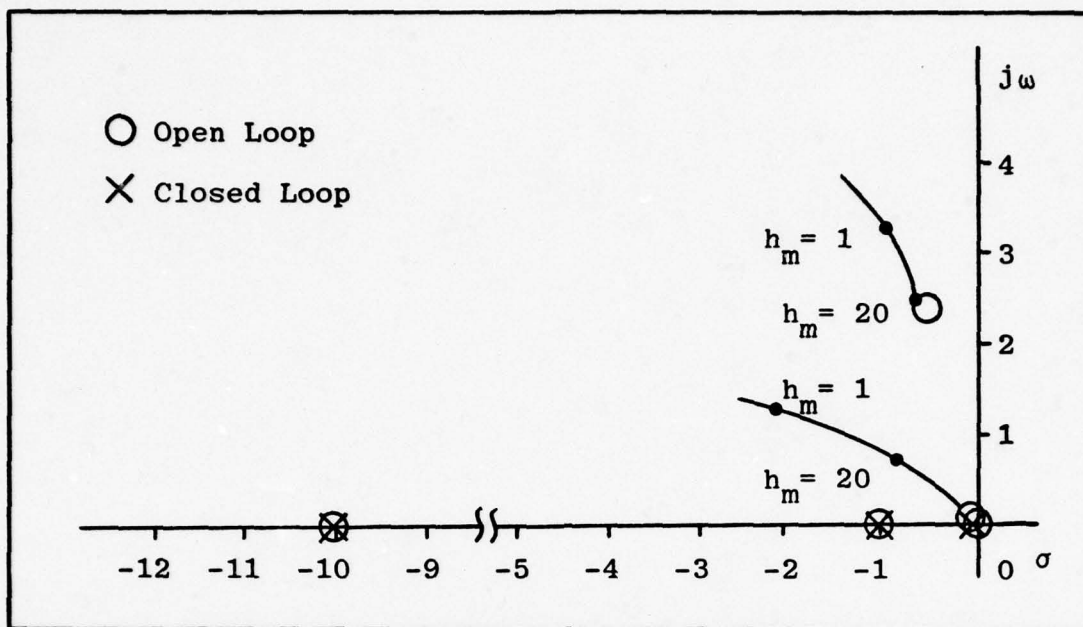


Figure 11. Root-locus as a function of state cost q_1 with $q_2 = 486.2$, $q_3 = 3.78E+08$, $q_4 = .0001$, $r_1 = 1459$, $r_2 = 6.25E-08$.

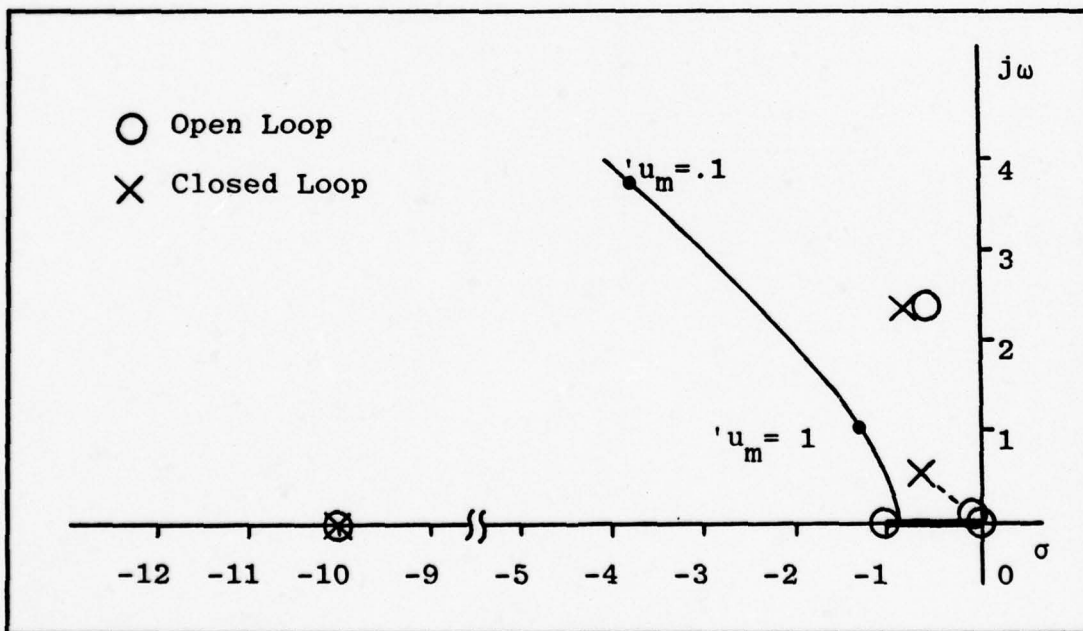


Figure 12. Root-locus as a function of state cost q_4 with $q_1 = .0025$, $q_2 = 486.2$, $q_3 = 3.78E+08$, $r_1 = 1459$, $r_2 = 6.25E-08$.

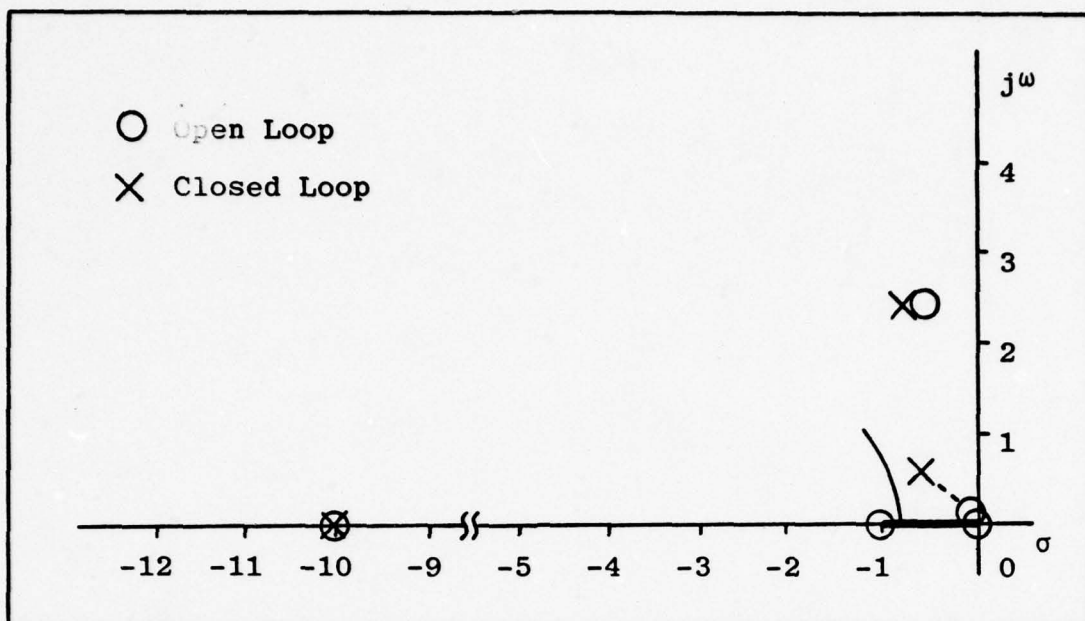


Figure 13. Root-locus as a function of control cost r_2 with $q_1 = .0025$, $q_2 = 486.2$, $q_3 = 3.78E+08$, $q_4 = .0001$, $r_1 = 1459$.

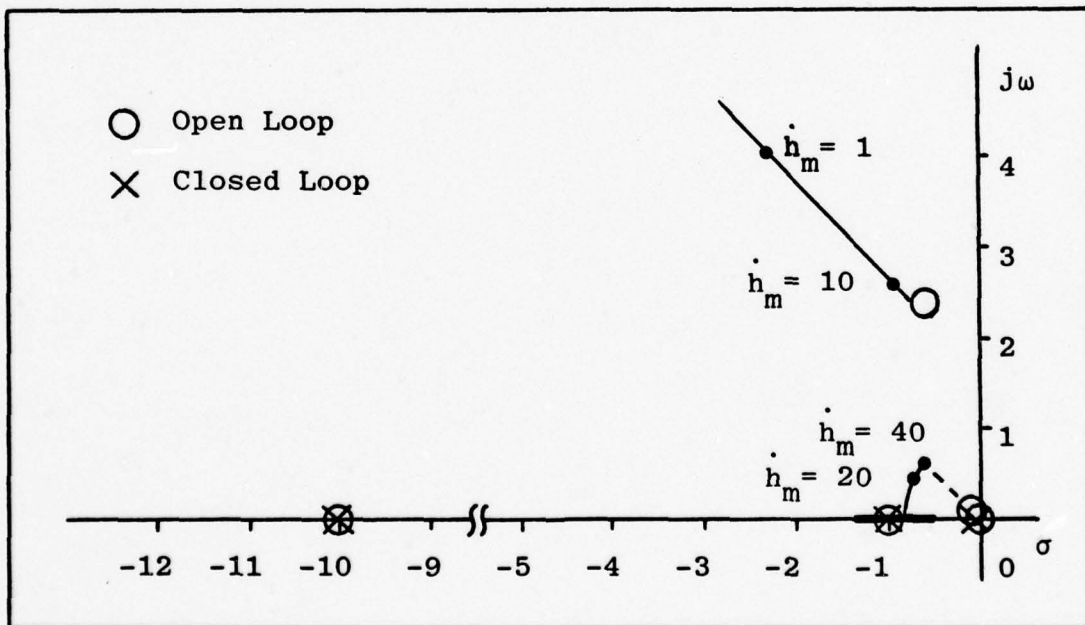


Figure 14. Root-locus as a function of state cost q_2 with $q_1 = .0025$, $q_3 = 3.78E+08$, $q_4 = .0001$, $r_1 = 1459$, $r_2 = 6.25E-08$.

either the parameter q_4 or r_2 . Since for this study it is desired to hold throttle cycling to a minimum, the closed loop location of the roots that correlate with the airspeed and thrust response will be established by the original value of q_4 equal to .0001. The parameter r_2 will be set equal to $6.25E-08$ which corresponds to 4000 pounds for ΔT_m . The 4000 pound figure is taken as ten per cent of the available military thrust at sea-level. Figure 15 shows the output cost matrix, \underline{Q} , the corresponding state cost matrix, \underline{S} , the control cost matrix, \underline{R} , and the feedback gain matrix, \underline{K} , for the above root locations. Figure 16 lists the eigensystem of the optimal closed loop system.

Analog Computer Simulation

The linearized longitudinal equations of motion developed in Chapter II were programmed on an analog computer. The basic aircraft response to a one degree elevator command of one second duration is shown in Figure 17. The response graphically displays the underdamped nature of the short-period response (damping ratio equal to .22). The control law was then implemented using the feedback gain matrix, \underline{K} , shown in Figure 15.

The closed loop system was evaluated for an initial condition on altitude deviation, h , airspeed deviation, u , and pitch deviation, θ . These initial conditions were applied individually and the response of the states observed to determine the "goodness" of the control law. As shown in Figures 18, 19, and 20, the state responses are well behaved for each of the initial conditions. As a side


```

OUTPUT COST MATRIX, Q .....
      .2500E-02      0.0      0.0      0.0
      0.0      .4862E+03      0.0      0.0
      0.0      0.0      .6720E+11      0.0
      0.0      0.0      0.0      .1000E-03

STATE COST MATRIX, S .....
      .1276E-02      .9367E-02      .2285E-01      0.0      .5530E+00      .4125E-06      0.0
      .9367E-02      .7525E-01      .1821E+00      -.5512E+00      .4406E+01      .3286E-05      0.0
      .2285E-01      .1821E+00      .4442E+00      0.0      .1075E+02      .8017E-05      0.0
      0.0      -.5512E+00      0.0      .4862E+03      0.0      0.0      0.0
      .5530E+00      .4406E+01      .1075E+02      0.0      .2601E+03      .1940E-03      0.0
      .4125E-06      .3286E-05      .8017E-05      0.0      .1940E-03      .1447E-09      0.0
      0.0      0.0      0.0      0.0      0.0      0.0      .2500E-02

CONTROL COST MATRIX, R .....
      .1459E+04      0.0
      0.0      .6250E-07

FEEDBACK GAIN MATRIX, K .....
      .8036E-03      -.1285E-02      .2019E+01      .4738E+00      -.7244E+00      .4041E-06      .1308E-02
      -.4325E+02      .1967E+01      -.4242E+04      -.1923E+05      .9433E+03      -.2972E-01      -.5677E+01

```

Figure 15. Output cost matrix, state cost matrix, control cost matrix, and feedback gain matrix.

CLOSED LOOP

EIGENVALUES

EIGENVECTORS

-3.797 ± j 3.435

-.684E-05 ± j .190E-02
-.177 ± j .383
.223E-02 ± j .565E-03
-.248E-03 ± j .374E-03
.246E-02 ± j .735E-03
1.000
.131E-01 ± j .213E-02

-.273 ± j .268

-.494E-02 ± j .158E-01
.855E-01 ± j .472E-01
.606E-04 ± j .170E-05
-.116E-03 ± j .108E-03
-.115E-03 ± j .610E-04
1.000
.263 ± j .433

-10.129

.243E-02
.927
-.113E-01
.111E-02
-.262E-01
-.373
-.517E-02

-.999

-.718E-03
.471E-04
-.554E-07
.554E-07
-.522E-07
1.000
-.177E-05

-.334E-01

-.246E-01
.326E-02
-.124E-06
.370E-05
-.368E-05
.9997
-.481E-04

Figure 16. Closed loop eigensystem.

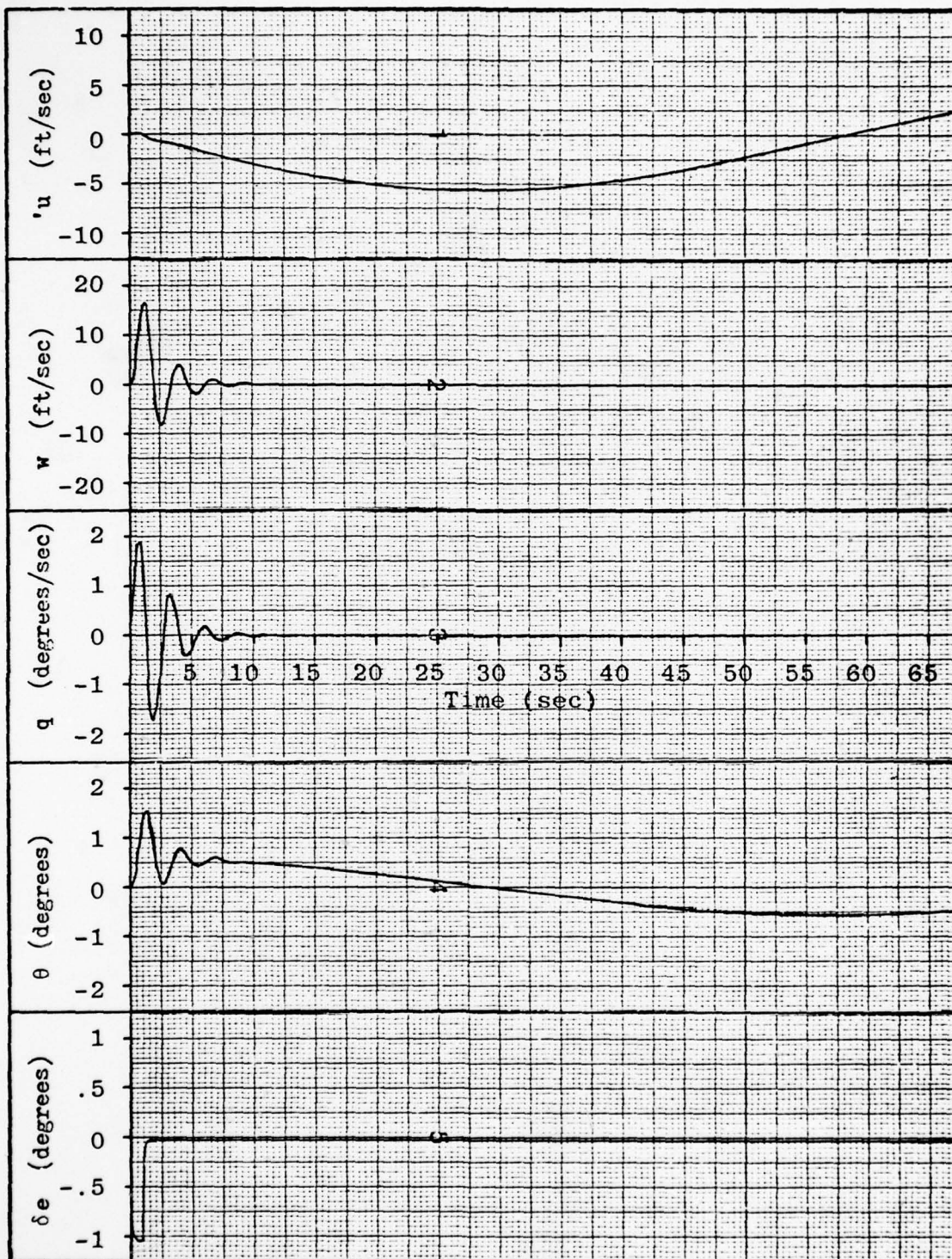


Figure 17. Aircraft open loop response to a one degree elevator command of one second duration.

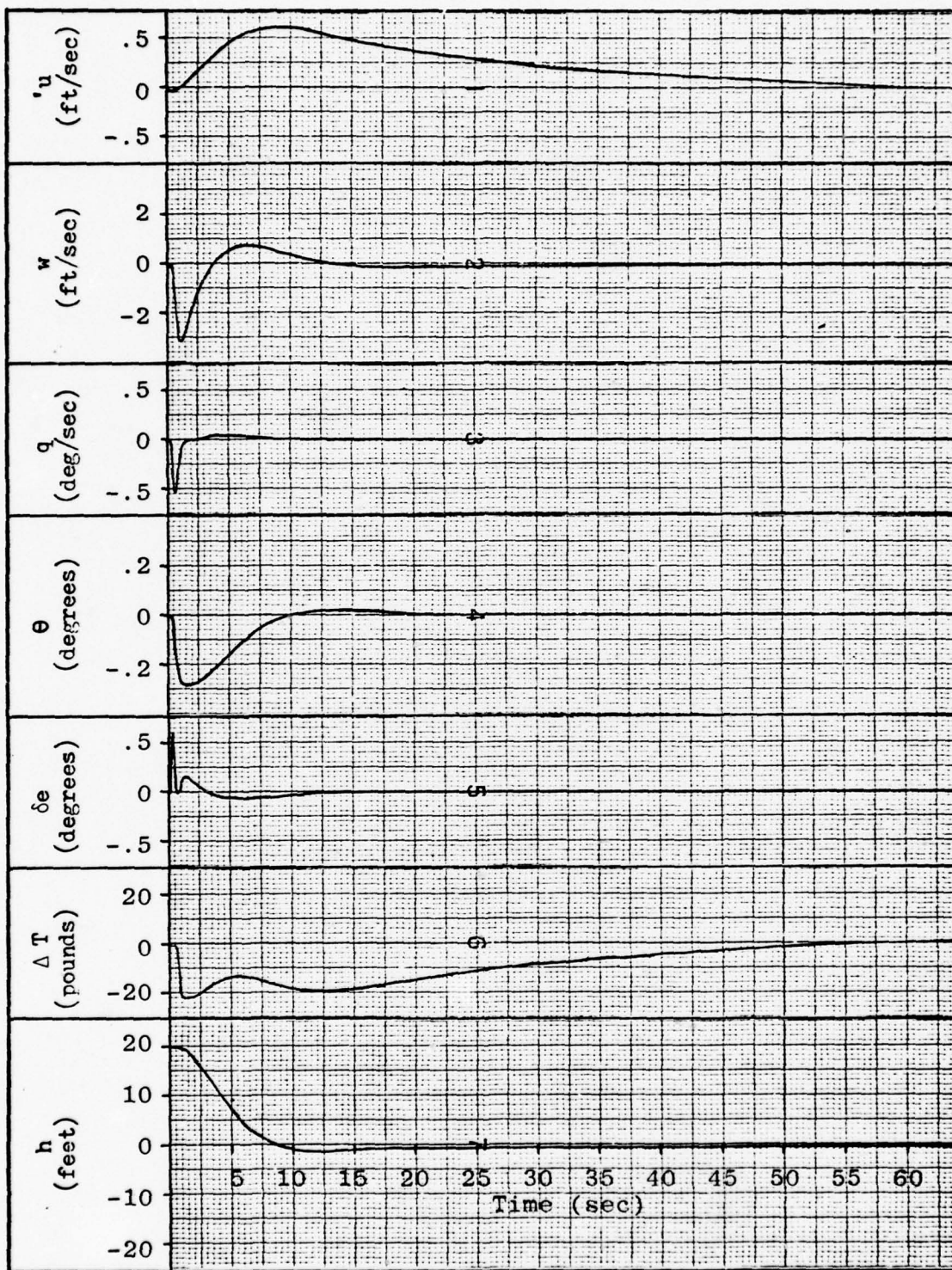


Figure 18. System closed loop response to an initial condition of 20 feet on the state variable h .

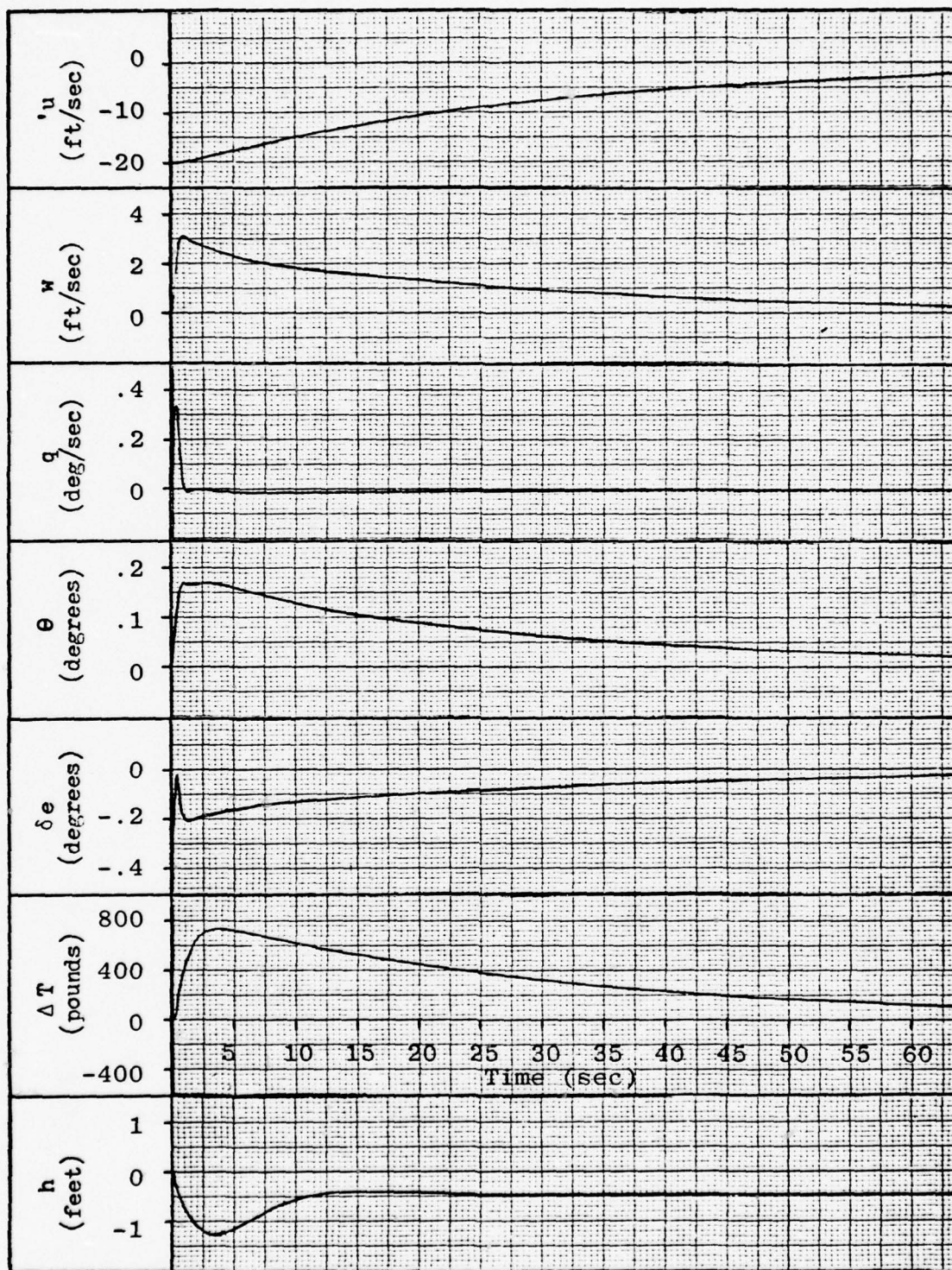


Figure 19. System closed loop response to an initial condition of -20 feet per second on the state variable u .

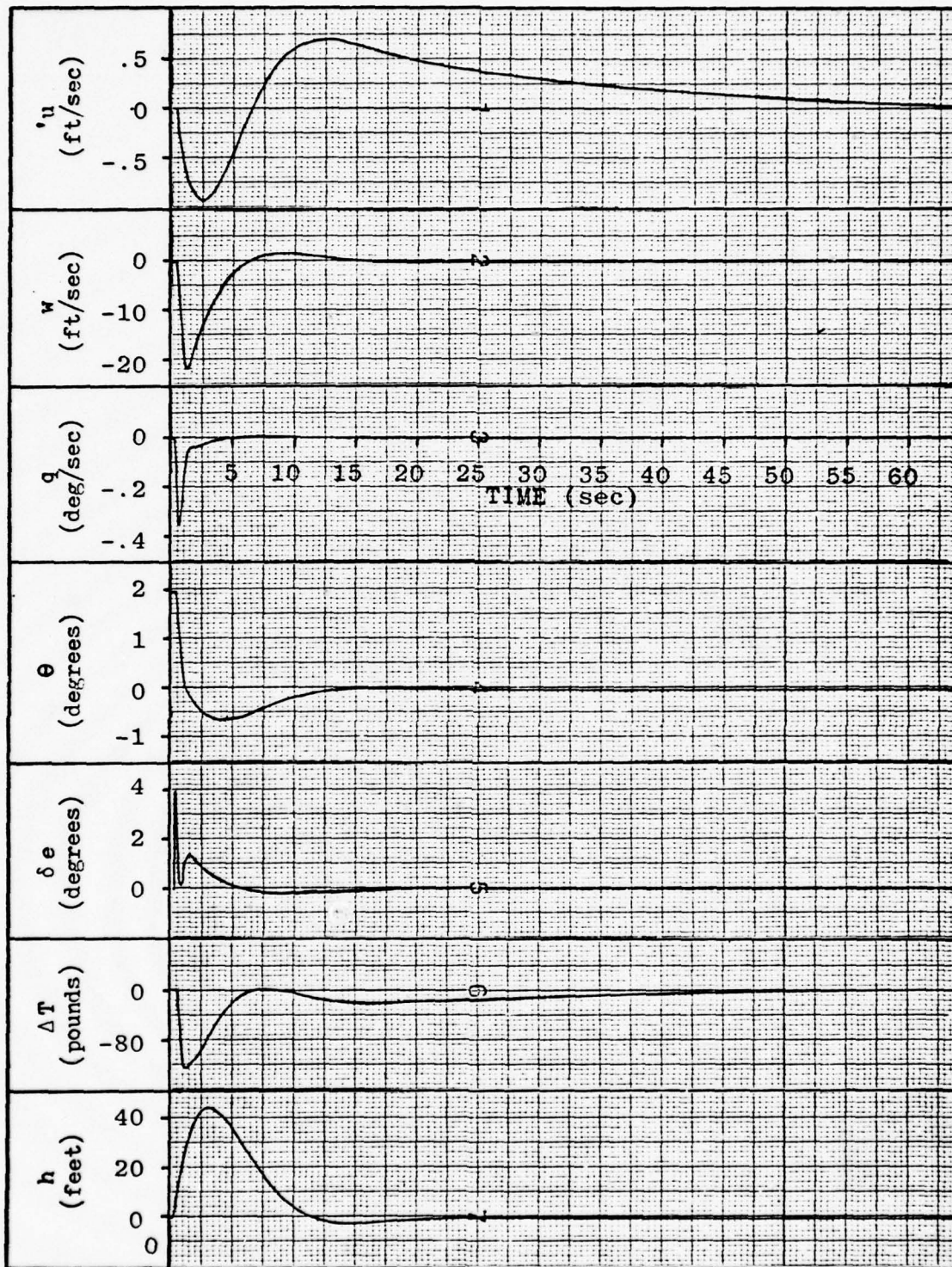


Figure 20. System closed loop response to an initial condition of two degrees on the state variable θ .

note of controller "goodness", the controller was modified to generate a C* response. To do this the following development was necessary.

C* Time History

The C* criteria was first proposed by the Boeing Aircraft Company (Ref 6) and was also explored as a handling qualities criteria in the Survivable Flight Control System study conducted in 1971 (Ref 10). C* is defined as

$$C^* = k_1 a_n + k_2 \dot{\theta} \quad (42)$$

where k_1 and k_2 are constants and a_n is normal acceleration. Normal acceleration can be approximated by

$$a_n \approx \frac{V_n \dot{\gamma}}{32.2} \quad (43)$$

where $\dot{\gamma}$ is the time rate of change of the flight path angle.

Also

$$\dot{\gamma} \approx \frac{\ddot{h}}{V_n} \quad (44)$$

thus

$$a_n \approx \frac{\ddot{h}}{32.2} \quad (45)$$

From equation (26)

$$\ddot{h} = -Z_u' u - Z_w w - Z_q q - Z_{\delta e} \delta e - Z_{\Delta T} \Delta T \quad (46)$$

therefore

$$C^* = \frac{k_1(\ddot{h})}{32.2} + k_2 q \quad (47)$$

The steady state relationship between q and a_n is

$$q_{ss} = \frac{a_{nss} (32.2)}{v_n} \quad (48)$$

If equal importance is placed on the steady state normal acceleration and pitch rate at a mid-range velocity such that

$$k_1 a_{nss} = k_2 q_{ss} \quad (49)$$

then the mid-range velocity is defined as the crossover velocity, v_{co} . Solving for k_1 yields

$$k_1 = \frac{k_2 (32.2)}{v_{co}} \quad (50)$$

and C^* becomes

$$C^* = \frac{k_2}{v_{co}} (\ddot{h}) + k_2 q \quad (51)$$

Defining a scaled C^* response as

$$C_n^* \equiv \frac{C^*}{k_2} (v_{co}) \quad (52)$$

then

$$C_n^* = -Z_u' u - Z_w w + (v_{co} - Z_q) q - Z_{\delta e} \delta e - Z_{\Delta T} \Delta T \quad (53)$$

It is now possible to obtain an equivalent C^* time history for the system based on a selection of the crossover velocity.

The control law for the system must first be modified so as not to penalize for a deviation in altitude or pitch. This is accomplished by setting the value of the feedback gain on these two states to zero. In addition, the C^* criteria is based on a short period approximation; thus, the

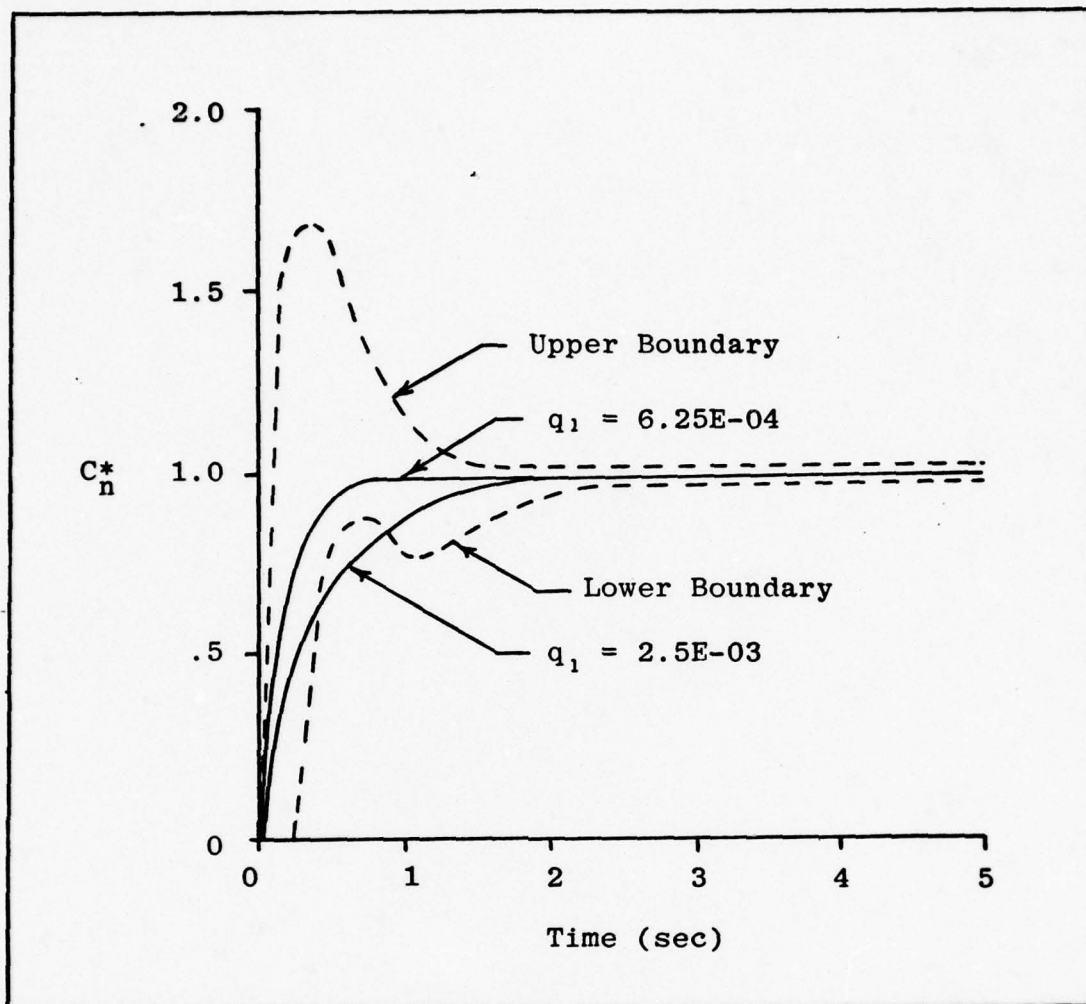


Figure 21. Normalized C_n^* response with $q_2 = 486.2$, $q_3 = 6.72 \text{ E}+10$, $q_4 = .0001$, $r_1 = 1459$, $r_2 = 6.23\text{E}-06$ for two values of cost parameter q_1 .

deviation in airspeed is defined to be zero. With these alterations made in the analog program, the C_n^* time history is shown in Figure 21 with C_n^* normalized to unity for the steady state. The system was connected in the command follower configuration and a step elevator command applied. The cross-over velocity was set equal to 400 feet per second.

As shown in Figure 21, the rise time for the C_n^* response is closely associated with the cost parameter q_1 . While the

cost matrices were chosen to provide a desirable state response for the regulator problem, it is interesting to note the "goodness" of the selection when evaluated against the C^* criteria.

Summary

The continuous deterministic regulator problem was solved to provide the state cost matrix and control cost matrix for the desired closed loop system. The selection of these matrices was based on the Cornell Aeronautical Laboratory "thumbprint" which specified the short period natural frequency and damping ratio. Once the selection of the matrices was completed, an analog computer simulation was accomplished to verify the "goodness" of the selection. The control law was then modified to yield a C_n^* response which was compared with the C^* criteria developed in the Survivable Flight Control System study (Ref 10). With the cost matrices determined, it is now possible to proceed with the discrete optimal regulator problem.

IV. Discrete Deterministic Regulator Problem

There are many different methods that can be used in designing a discrete compensator for a continuous system as explained in Chapter I. They are normally broken down into two categories: (1) digitization of a compensator designed in the continuous domain (s -plane); or, (2) the direct design of the compensator in the discrete domain (z - or w -plane). The direct digital design state space approach has the advantages of not introducing errors due to approximating the zero order hold as in the digitization procedure and the state space approach easily handles multi-input multi-output systems.

In this chapter the discrete deterministic regulator problem will be solved as a function of sample rate. The minimum acceptable sample rate will be based on the effect the sample rate has on the closed loop roots. Katz and Powell developed a computer program, DISCUS, for the solution of the discrete regulator problem (Ref 5). The calculation of the regulator is based on eigenvector decomposition of the related state-costate Hamiltonian matrix similar to the earlier work by Bryson and Hall for the continuous problem (Ref 9). Included in the DISCUS program are subroutines for discretizing a continuous performance index and an associated continuous plant. Thus, the state cost and control cost matrices developed in Chapter III can be used in the discrete problem. While it is possible to define the cost matrices directly in the discrete domain by the use of DISCUS, the insight afforded by the continuous domain would be lost.

Discretization of the Continuous Plant

The discrete formulation of a linear, continuous, differential system can be thought of as the solution in the time domain from one point in time to another. The state model of a continuous system is given by (repeated from Chapter I)

$$\dot{\underline{x}} = \underline{A} \underline{x} + \underline{B} \underline{u} \quad (1)$$

$$\underline{y} = \underline{C} \underline{x} \quad (2)$$

The solution to equation (1) is

$$\underline{x} = \exp \underline{A}(t - t_0) \underline{x}_0(t_0) + \int_{t_0}^t \exp \underline{A}(t - \tau) \underline{B} \underline{u}(\tau) d\tau \quad (54)$$

Assuming that the inputs are held constant over intervals of T seconds, the input $\underline{u}(t)$ is of the form

$$\underline{u}(t) = \underline{u}(kT), \quad kT \leq t < (k+1)T \quad (55)$$

The initial condition at the beginning of the interval $\{kT, (k+1)T\}$ is

$$\underline{x}(t_0) = \underline{x}(kT) \quad (56)$$

To determine $\underline{x}(t)$ at the end of the interval

$$t_0 = kT \quad (57)$$

$$t = (k+1)T \quad (58)$$

is substituted into equation (54). Thus

$$\underline{x} \{(k+1)T\} = \exp \underline{A}T \underline{x}(kT) + \int_{kT}^{(k+1)T} \exp \underline{A}\{(k+1)T - \tau\} \underline{B} \underline{u}(kT) d\tau \quad (59)$$

Since the input $\underline{u}(kT)$ is constant for the integration interval and the integration is valid for all k , by making the change of variable $t = (k+1)T - \tau$ equation (59) becomes

$$\underline{x} \{(k+1)T\} = \exp \underline{A}T \underline{x}(kT) + \int_0^T \exp \underline{A}t \underline{B} dt \cdot \underline{u}(kT) \quad (60)$$

Provided the sampling interval T is constant and the \underline{A} and \underline{B} matrices are time invariant, then

$$\exp \underline{A}\tau = \underline{\phi}(\tau) \quad 0 \leq \tau \leq T \quad (61)$$

$$\text{and} \quad \int_0^T \exp \underline{A}t \underline{B} dt = \underline{G}(T) \quad (62)$$

When $\tau = T$, $\underline{\phi}$ and \underline{G} are constant matrices whose elements are functions of the sampling interval T . In conclusion, the discrete state model for a continuous system with a piecewise constant input is

$$\underline{x} \{(k+1)T\} = \underline{\phi}(T) \underline{x}(kT) + \underline{G}(T) \underline{u}(kT) \quad (63)$$

$$\underline{y}(kT) = \underline{C} \underline{x}(kT) \quad (64)$$

Discretization of a Continuous Performance Index

A continuous quadratic performance index

$$J = \frac{1}{2} \int_0^t (\underline{x}^T \underline{S} \underline{x} + \underline{u}^T \underline{R} \underline{u}) d\tau \quad (65)$$

can be transformed into a discrete version

$$J = \sum_{i=0}^{N-1} \begin{bmatrix} \underline{x}_i^T & \underline{u}_i^T \end{bmatrix} \begin{bmatrix} \underline{A}_{11} & \underline{A}_{12} \\ \underline{A}_{21} & \underline{A}_{22} \end{bmatrix} \begin{bmatrix} \underline{x}_i \\ \underline{u}_i \end{bmatrix} \quad (66)$$

where $N = t/T$ by the following manipulations. Equation (65) can be written as

$$J = \sum_{i=0}^{N-1} \int_{iT}^{(i+1)T} (\underline{x}^T \underline{S} \underline{x} + \underline{u}^T \underline{R} \underline{u}) d\tau \quad (67)$$

$$\text{since } \underline{x}(\tau) = \underline{\Phi}(\tau-iT) \underline{x}_i + \underline{G}(\tau-iT) \underline{u}_i \quad (68)$$

$$\text{where } iT \leq \tau \leq (i+1)T$$

then

$$\int_{iT}^{(i+1)T} (\underline{x}^T \underline{S} \underline{x} + \underline{u}^T \underline{R} \underline{u}) d\tau = \begin{bmatrix} \underline{x}_i^T & \underline{u}_i^T \end{bmatrix} \begin{bmatrix} \underline{A}_{11} & \underline{A}_{12} \\ \underline{A}_{21} & \underline{A}_{22} \end{bmatrix} \begin{bmatrix} \underline{x}_i \\ \underline{u}_i \end{bmatrix} \quad (69)$$

where

$$\underline{A}_{11} = \int_0^T \underline{\Phi}^T(\tau) \underline{S} \underline{\Phi}(\tau) d\tau \quad (70)$$

$$\underline{A}_{22} = \int_0^T \{ \underline{G}^T(\tau) \underline{S} \underline{G}(\tau) + \underline{R} \} d\tau \quad (71)$$

$$\underline{A}_{12} = \int_0^T \underline{\Phi}^T(\tau) \underline{S} \underline{G}(\tau) d\tau \quad (72)$$

$$\underline{A}_{21} = \underline{A}_{12}^T \quad (73)$$

The DISCUS program has subroutines based on the above developments for discretizing a continuous plant and a continuous performance index. The closed loop roots and discrete feedback gain matrix for the regulator problem can now be obtained.

Discrete System Closed Loop Roots

Using the DISCUS program, the discrete regulator problem was solved at various sample rates. The continuous state and control cost matrices of Chapter III, Figure 15, were used in the performance index along with the sample rates of interest. The resulting closed loop root movement for the

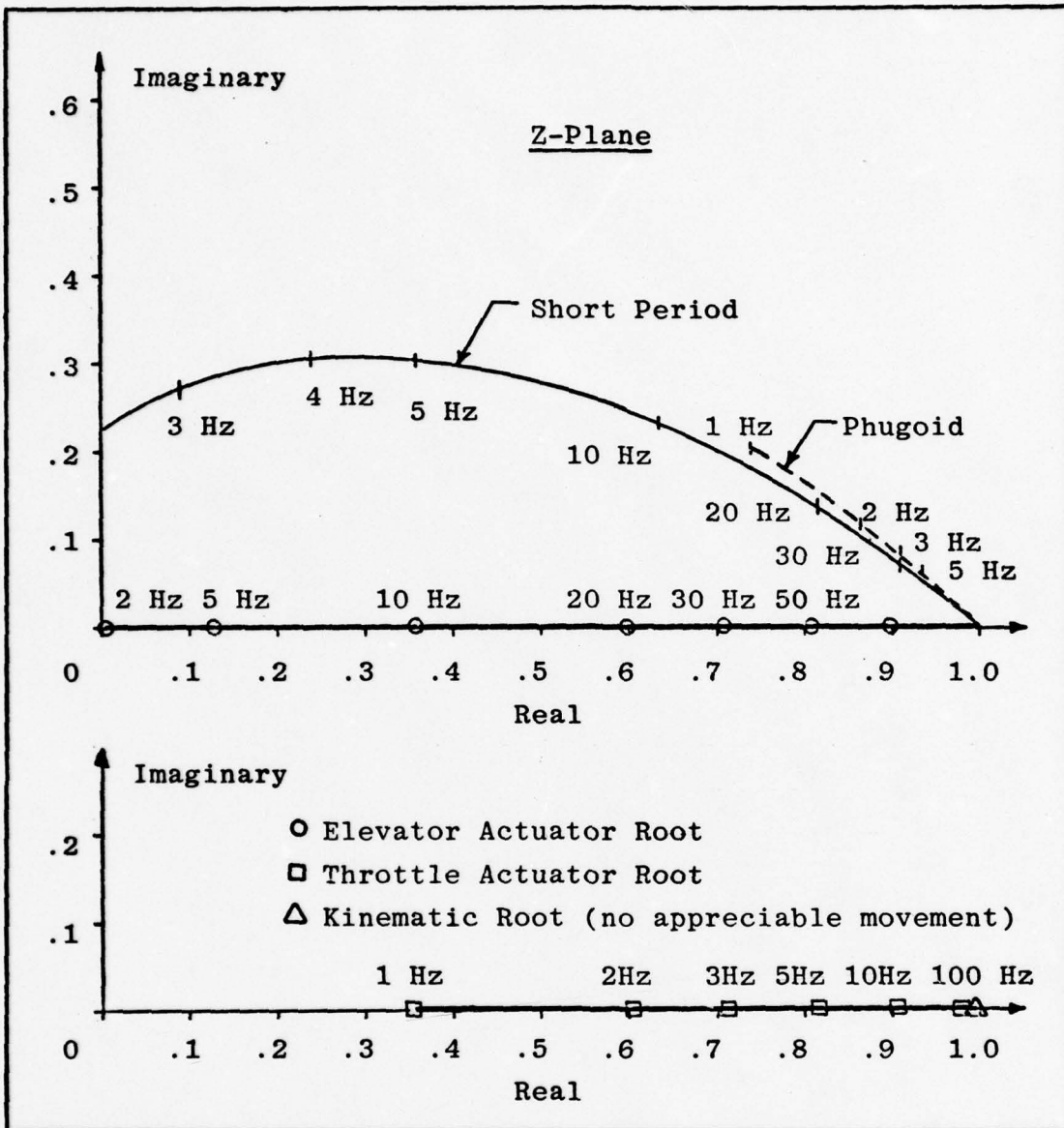


Figure 22. Discrete closed loop root movement as a function of sample rate.

discrete roots (z-plane) is shown in Figure 22. The equivalent continuous root movement (s-plane) is shown in Figure 23.

Z-Plane Roots. As illustrated in Figure 22, the discrete closed loop root movement for the short period and phugoid modes forms loci with a damping ratio of approximately .7.

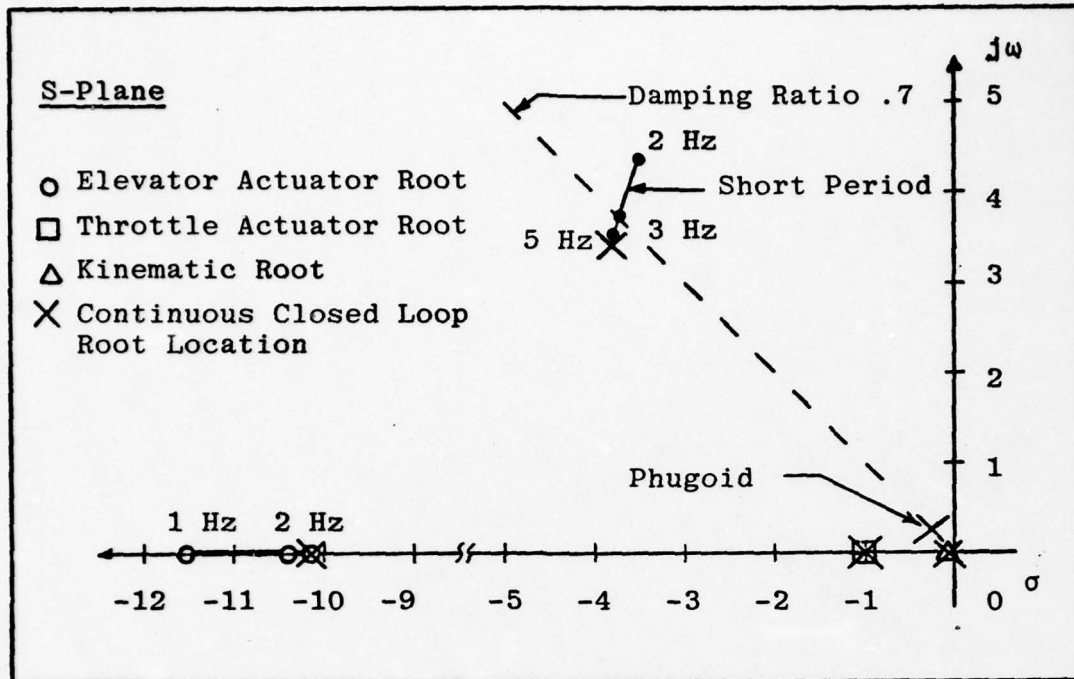


Figure 23. Equivalent s-plane discrete closed loop root location as a function of sample rate.

This is true of the short period root movement down to a frequency of five hertz. This should be the case, since the dominant roots have a damped natural frequency of 3.44 radians per second (.55 Hz). As long as the system is being sampled at a rate at least ten times the dominant mode, the effects of the sampling should be minimal. When the sample rate is reduced below five hertz, the locus diverges more and more from the .7 damping ratio indicating the effects of sampling at less than ten times the dominant mode. For the system under study, it has been assumed that the aircraft is a rigid body; thus, the body bending modes have been ignored. The body bending modes may be such that the five hertz sample rate would not excite them. If this is not the case the rate of sampling would have to be adjusted. This particular facet of

of the problem will not be explored further by this study.

Equivalent S-Plane Roots. The equivalent s-plane roots are determined by the relationship

$$z = e^{sT} \quad (74)$$

thus $s = (\ln z)/T \quad (75)$

where T is the sampling period and s is the Laplace operator. The periodic nature of equation (75) must be realized to fully describe the equivalent s-plane roots. Since for a complex variable

$$\ln z = \ln |z| + j \arg z \pm 2n\pi j \quad (76)$$

for $n = 0, 1, 2, \dots$

the complex natural logarithm is infinitely many valued. Figure 23 indicates only the portion of the primary strip that contains the principle value of the logarithm. It is pointed out that to use an equivalent s-plane mapping, the effects of the folded roots, the roots indicated by the $\pm 2n\pi j$ term in the complex logarithm, must also be considered. At a sample rate of five hertz, the primary strip extends from -15.7 to $+15.7$ radians per second. Thus, the nearest folded root is located at $-3.8 \pm j 28$. This is far enough removed from the dominant roots to have minimal effect on the system. This is not true of a two hertz sample rate since the primary strip has moved into ± 6.28 radians per second. At two hertz the nearest folded roots are located

at $-3.8 \pm j 9.1$ and may degrade the response of the system. It is also shown in Figure 23 that at five hertz the system closed loop root location closely approximates the continuous root location.

Hybrid Regulator Simulation

The linear perturbation model developed in Chapter II was programmed on an analog computer and the control laws were implemented on a Xerox Sigma 7, 112K, 32-bit word computer. The systems were interfaced using ± 100 volt, 15 bit, analog to digital converters and ± 100 volt, 15 bit digital to analog converters.

The closed loop system in the form of the discrete regulator was evaluated for an initial condition on altitude deviation, h , airspeed deviation, u , and pitch deviation, θ . The initial conditions were applied individually, as in the evaluation of the continuous regulator of Chapter III, using sample rates from 100 hertz to 2 hertz. The states were observed to determine the effects of the sampling in the time response. As expected, at the higher sample rates no discernable difference from the continuous system could be observed. As the sample rate was lowered below 20 hertz, the discrete nature of the control became apparent. A slight ripple was observable in some of the states. While this ripple, or noise, was not predictable on the basis of the z - and s -plane root analysis, it is pointed out that these analysis tools do not take into account the finite word length constraint of the digital computer and the associated interfacing. While this computer had a word length of 32 bits, the relatively small

word length of the analog to digital and digital to analog converters introduced a round off error that was evident at the lower sample rates. At the higher rates of sampling, the noise was effectively filtered by the elevator and throttle actuators.

Figure 24 shows the system state response at five hertz to an initial condition of 20 feet on the state variable h . The noise introduced by the discrete system is most evident in the state variable ΔT . The noise appears to have a maximum strength of plus or minus one pound - which is small indeed. The regulator response to an initial condition on the state variable u is shown in Figure 25. The noise is no longer apparent in the ΔT state due to the scaling of the variable for recording. The noise is noticeable in θ , q , and δe . The noise has a maximum strength of approximately ± 0.01 degree in the elevator deflection, ± 0.05 degree in pitch, and ± 0.01 degree per second in pitch rate. The commanded elevator deflection is included in Figure 25 to illustrate the discrete nature of the noise introduced by the digital process. Figure 26 depicts the discrete regulator response at a sample rate of five hertz to an initial condition of two degrees on the state variable θ . The noise is suppressed in this figure due to the lower amplifications required in scaling the variables for recording.

The state variable closed loop responses at a sample rate of two hertz for the same initial conditions are shown in Figures 27, 28, and 29. The magnitude of the noise has increased since the error introduced in the control law has longer to

act in the system before the system is again sampled.

Summary

Direct digital design has the advantage of not introducing errors into a discrete system since the zero order hold is accounted for precisely. The state space approach lends itself nicely to multiple input, multiple output systems and, through the use of optimal control techniques, the design engineer can readily come to grips with very demanding control problems. It was shown in this chapter how an optimal regulator problem was discretized. The effects of sample rate on the system were then examined. The finite word length of a digital system was shown to produce the equivalent of a noise being introduced into the system. The sampling rate of five hertz was shown to be high enough to form the desired controls. In the following chapter, the task of terrain following will be explored using the regulator that has thus far been developed.

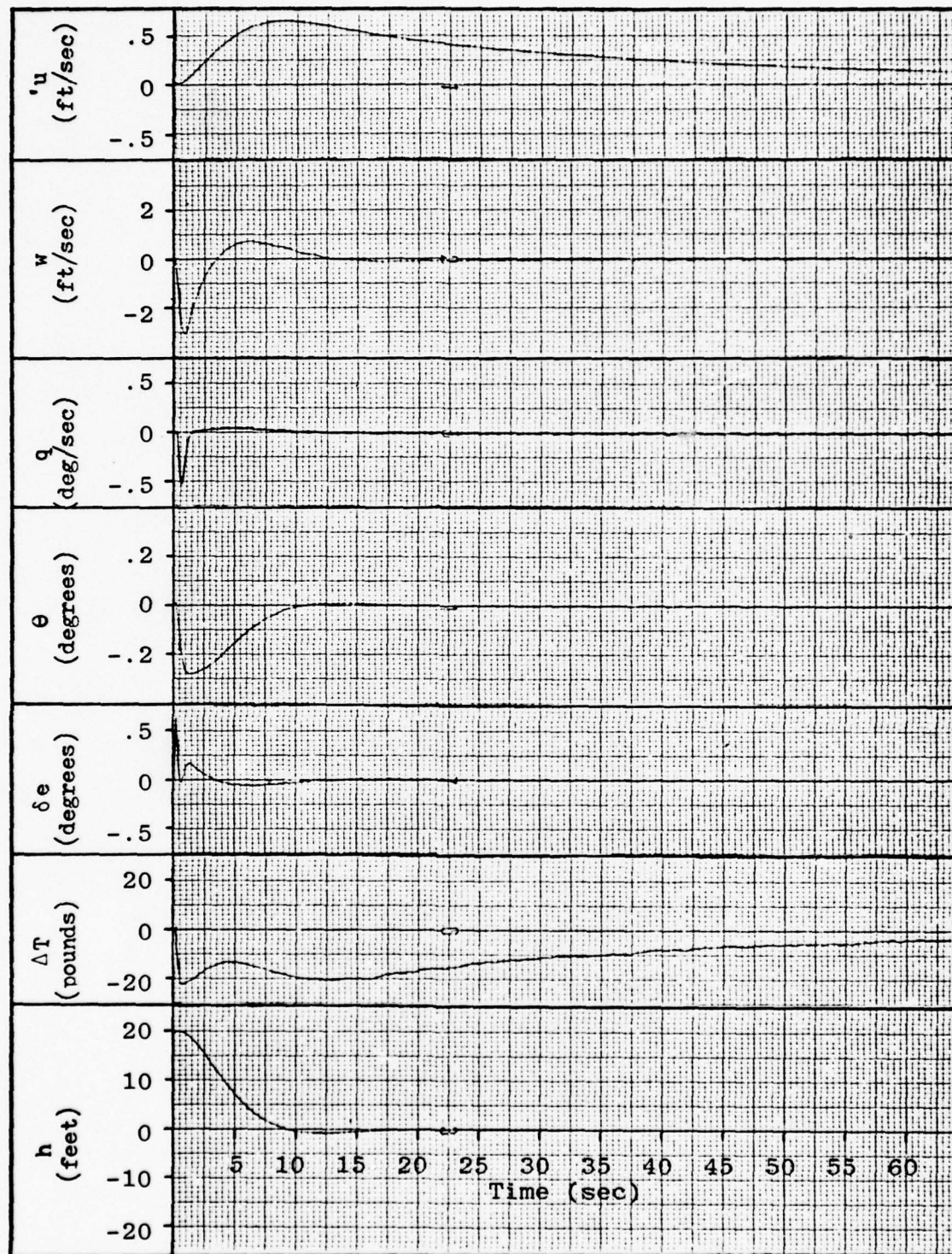


Figure 24. System closed loop response to an initial condition of 20 feet on the state variable h using a five hertz sample rate.

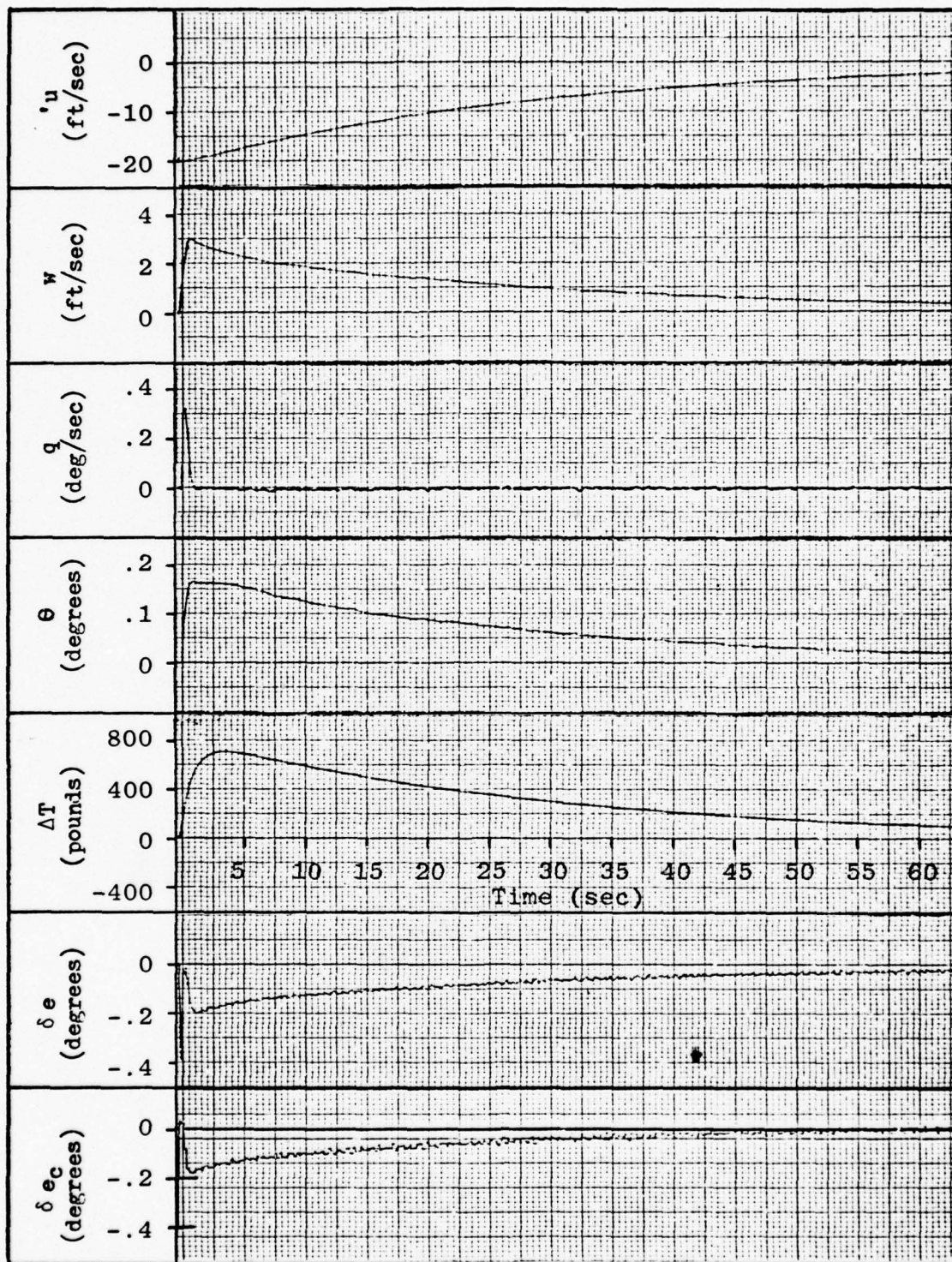


Figure 25. System closed loop response to an initial condition of -20 feet per second on the state variable 'u' using a five hertz sample rate.

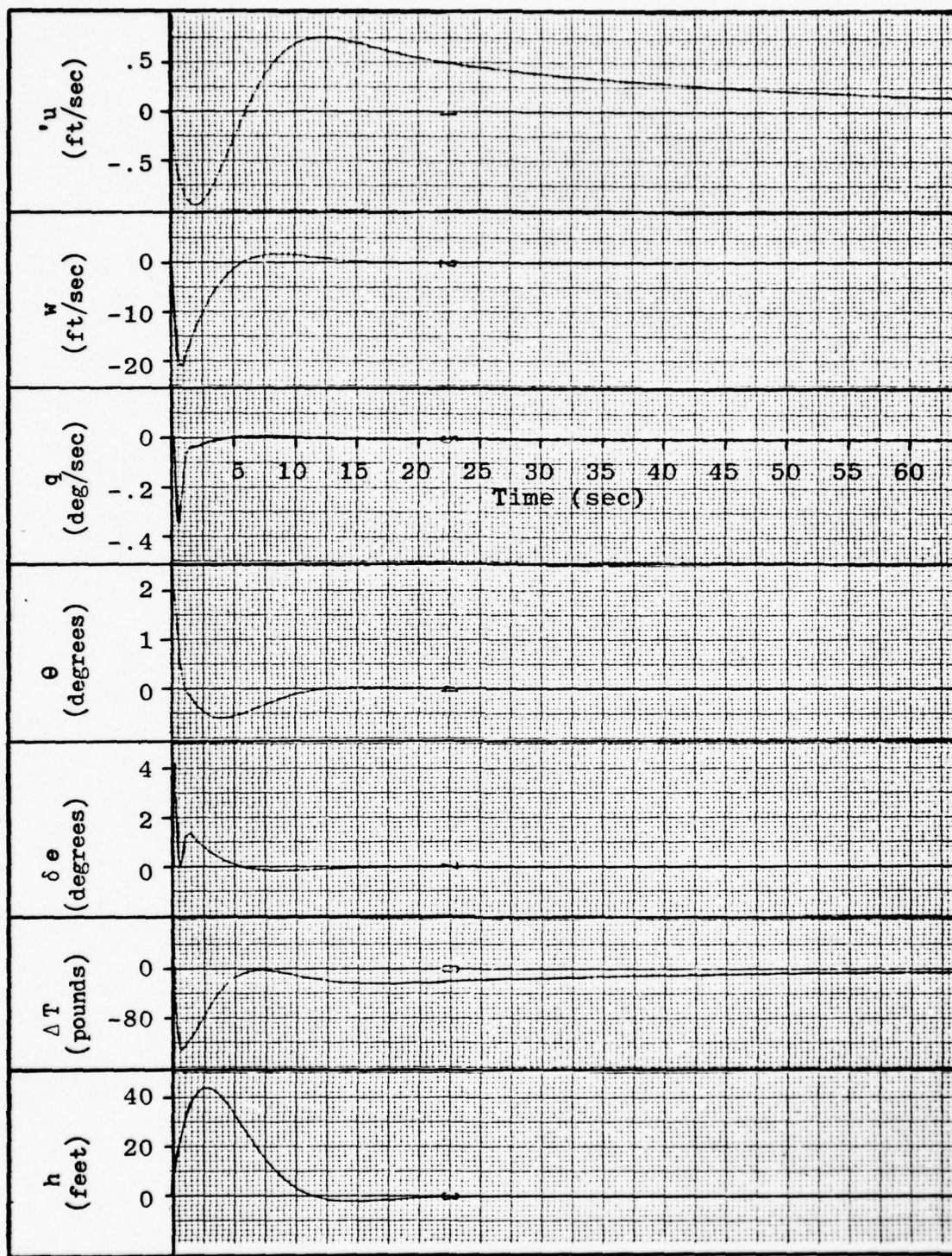


Figure 26. System closed loop response to an initial condition of two degrees on the state variable θ using a sample rate of five hertz.

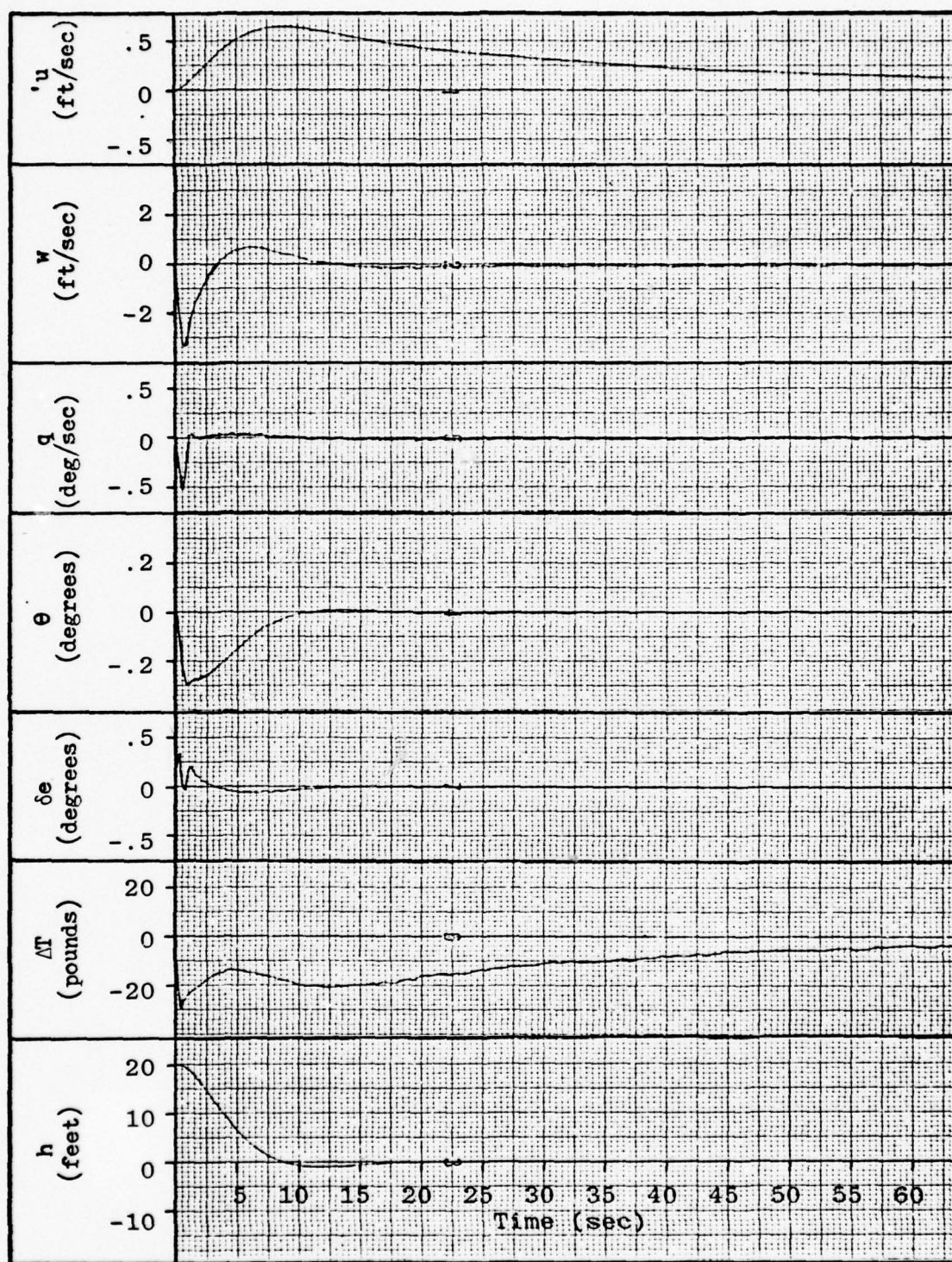


Figure 27. System closed loop response to an initial condition of 20 feet on the state variable h using a two hertz sample rate.

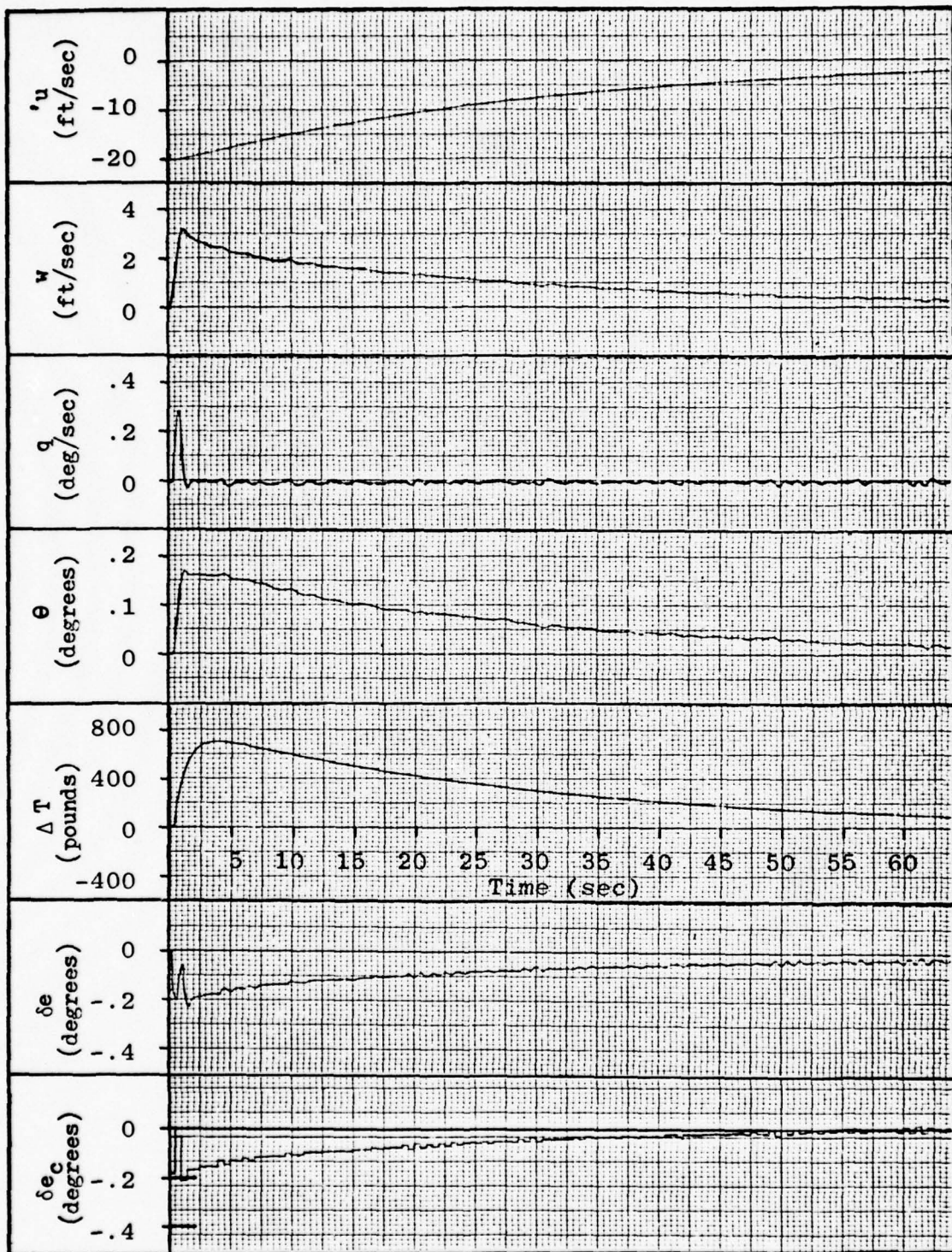


Figure 28. System closed loop response to an initial condition of -20 feet per second on the state variable 'u' using a two hertz sample rate.

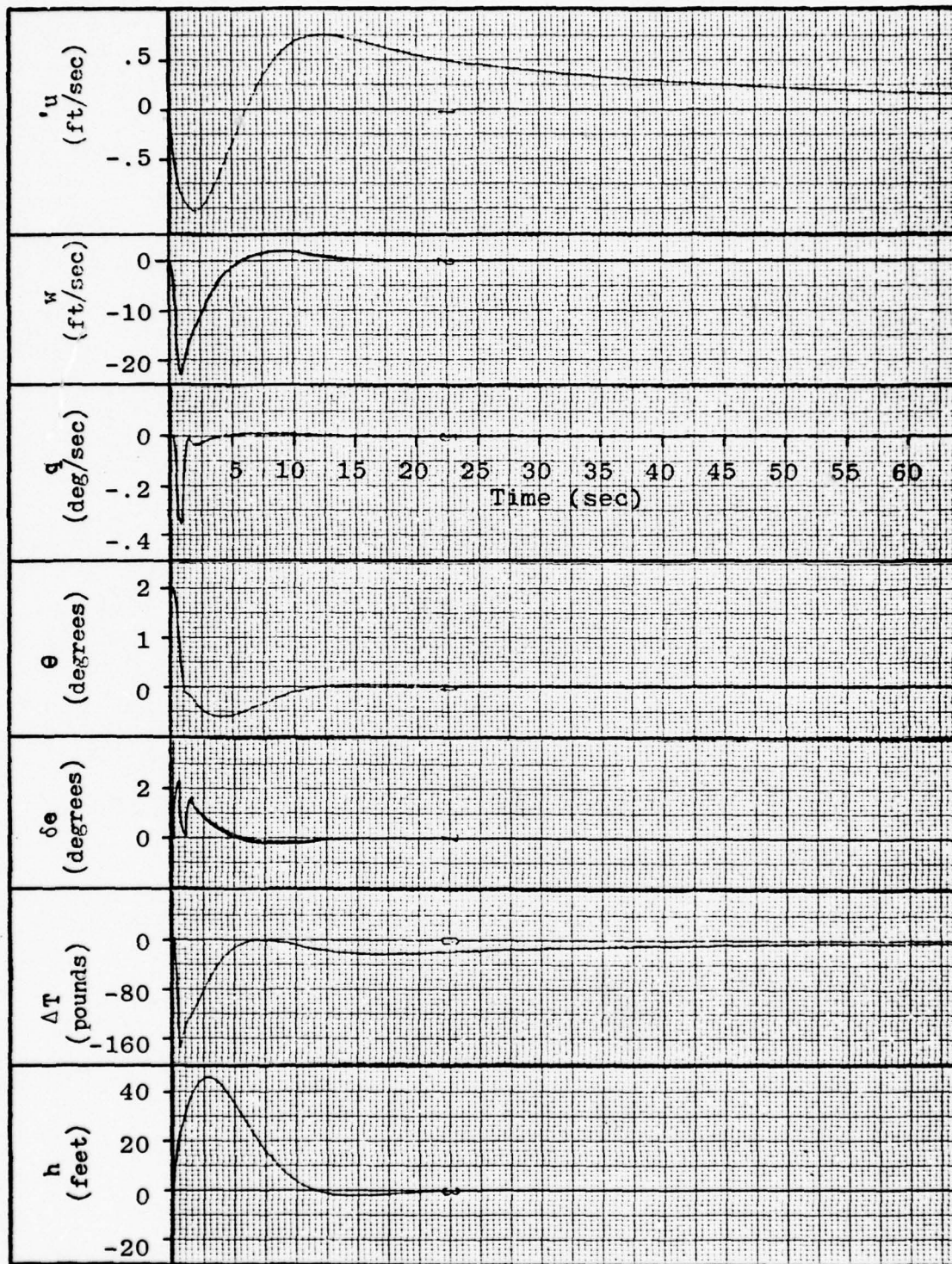


Figure 29. System closed loop response to an initial condition of two degrees on the state variable θ using a sample rate of two hertz.

V. The Terrain Following Task

In addition to the regulator developed in the previous chapters, it is necessary to derive the reference command generator and to obtain the desired path information in order to implement the system for the terrain following task. For the purpose of this study, the desired path over the terrain is assumed to be generated by an optimal cubic spline algorithm (Ref 11). The algorithm stores the desired altitude and the first derivative of altitude with respect to horizontal range indexed at prescribed range intervals. The higher derivatives of the path could also be stored but at an additional cost in required memory. This chapter will illustrate one method of reconstructing the desired path and path derivatives. Using the reconstructed path information, the reference commands and reference states are generated.

A change of notation is required since the total states and commands are the quantities of interest. From this point on in the thesis, the notation will refer to the total variable instead of the perturbation about the nominal condition as used previously. In the later portion of the chapter, the total system is evaluated through the use of a hybrid computer. A development of the non-linear aircraft longitudinal equations of motion is included in Appendix A. These equations were programmed on the analog portion of the hybrid system to serve as the truth model for the system under study. Included in Appendix B is a computer program REFCOM, developed to reconstruct the path and furnish the commands and reference

states. The feedback gain quantities for five of the sample rates employed are listed in Appendix C.

Path Reconstruction

It is shown in the literature (Ref 11; 152-157) how a cubic spline curve may be reconstructed and that derivation will not be repeated here. The required difference equations to perform this reconstruction from a known altitude, slope, and range are

$$h_d(\sigma) = h(k) + \sigma^2(3 - 2\sigma)\{h(k+1) - h(k)\} + \{(\sigma - 2\sigma^2 + \sigma^3)h'(k) + (\sigma^3 - \sigma^2)h'(k+1)\}\Delta R \quad (77)$$

$$h'_d(\sigma) = \frac{6\sigma}{\Delta R}(1 - \sigma)\{h(k+1) - h(k)\} + \{(1 - 4\sigma + 3\sigma^2)h'(k) + (3\sigma^2 - 2\sigma)h'(k+1)\} \quad (78)$$

$$h''_d(\sigma) = \frac{6(1 - 2\sigma)}{(\Delta R)^2} \{h(k+1) - h(k)\} + \frac{2}{\Delta R} \{(3\sigma - 2)h'(k) + (3\sigma - 1)h'(k+1)\} \quad (79)$$

$$h'''_d(\sigma) = \frac{-12}{(\Delta R)^2} \{h(k+1) - h(k)\} + \frac{6}{(\Delta R)^2} \{h'(k) + h'(k+1)\} \quad (80)$$

where σ is the non-dimensional range variable defined by

$$\sigma = \frac{R - R(k)}{\Delta R} \quad (81)$$

The variable R is the current range and ΔR is the dimensional range increment expressed by

$$\Delta R = R(k+1) - R(k) \quad (82)$$

The primes in equations (77) through (80) indicate the first through third derivatives of altitude, h , with respect to horizontal range. The parenthetical terms (k) and $(k+1)$ denote the current interval of operation as defined by the range variable R . Thus, the path is completely reconstructed for any range given the discrete range points $R(k)$ and $R(k+1)$, along with the slope at these points, $h'(k)$ and $h'(k+1)$, and the path altitude at these points, $h(k)$ and $h(k+1)$. It is now necessary to define the reference command generator.

Reference Command Generator

The reference command generator computes the desired input commands and reference states for use in the command follower system of Chapter I. A simple form of constant energy control is applied to determine the desired forward velocity, V_d . Since the energy of the system is held constant over the path legs, the resulting control system does not require a constant velocity. Throttle cycling is minimized and engine life increased. The desired energy level for each leg could be either calculated using apriori knowledge of the terrain or updated for each path leg based on the terrain of the previous leg and the required time over the path end point. The length of each path leg would be determined by the nature of the mission and the required tolerance in the time over target. If, due to navigational restraints, a constant air-speed controller were desired, the reference generator could be greatly simplified. The following is one means of deriving

a constant energy reference command generator.

Desired Velocity. The energy, E , of the center of mass required for a path leg can be defined by the sum of the kinetic and potential energies. The following represents this relationship

$$E = \frac{1}{2} mV^2 + mgh \quad (83)$$

If mass, m , is assumed constant, a scaled version of total energy can be obtained. Dividing both sides of the energy equation by a scaling factor equal to mass, the energy relationship becomes

$$E_o = \frac{1}{2} V_o^2 + gh_o \quad (84)$$

where V_o is the average forward velocity required to achieve the time over the path leg end point and h_o is mean path altitude. The average forward velocity is equivalent to the nominal velocity, V_n , used in the derivation of the feedback gain quantities in the previous chapters. The relationship for the desired velocity becomes

$$V_d = \sqrt{2(E_o - gh_d)} \quad (85)$$

where h_d is the desired path altitude provided by the path generator. The desired velocity and its associated derivatives are required in the development of the reference states and controls. The d subscript indicating a desired quantity will be dropped from this point on in the derivation except where needed for clarity. Since E_o is constant, the

first derivative of desired velocity is

$$\dot{V} = - \frac{gh}{V} \quad (86)$$

The path generator furnishes the spacial derivatives of altitude and these derivatives are related to the time derivative by

$$\begin{aligned} \dot{h} &= \frac{dh}{dR} \cdot \frac{dR}{dt} \\ &= h' V \cos \gamma \end{aligned} \quad (87)$$

where

$$h' = \frac{dh}{dR} \quad (88)$$

and

$$\frac{dR}{dt} = V \cos \gamma$$

The term γ is the desired flight path angle. Substituting the above value for \dot{h} into equation (86), \dot{V} becomes

$$\dot{V} = - g h' \cos \gamma \quad (90)$$

Since

$$h' = \tan \gamma \quad (91)$$

an equivalent expression for the derivative of desired velocity is

$$\dot{V} = - g \sin \gamma \quad (92)$$

Taking the second derivative yields

$$\ddot{V} = - g \dot{\gamma} \cos \gamma \quad (93)$$

Since

$$\gamma = \arctan h' \quad (94)$$

$$\text{then} \quad \dot{\gamma} = \frac{1}{1 + (h')^2} \frac{dh'}{dt} \quad (95)$$

Using the further relationships

$$(h')^2 = \tan^2 \gamma = \frac{\sin^2 \gamma}{\cos^2 \gamma} \quad (96)$$

$$\text{and} \quad \frac{dh'}{dt} = h'' V \cos \gamma \quad (97)$$

$$\dot{\gamma} \text{ becomes} \quad \dot{\gamma} = h'' V \cos^3 \gamma \quad (98)$$

$$\text{Defining} \quad K = h'' \cos^3 \gamma \quad (99)$$

$$\text{then} \quad \dot{\gamma} = K V \quad (100)$$

And the second derivative of the flight path angle is

$$\ddot{\gamma} = \dot{K} V + K \dot{V} \quad (101)$$

$$\text{where} \quad \dot{K} = V(h''' \cos^4 \gamma - 3K^2 h') \quad (102)$$

Substituting the value of $\dot{\gamma}$ into equation (93), \ddot{V} becomes

$$\ddot{V} = -g K V \cos \gamma \quad (103)$$

The desired velocity and its derivatives have, thus, been defined in terms of the available quantities from the path generator. It is next necessary to derive the reference angle of attack, α_r , and elevator reference command, δe_r . Once this is accomplished, the remaining elements of the state reference vector can be derived.

Reference Angle of Attack and Elevator Command. In order to solve for the reference angle of attack and elevator com-

mand, it is necessary to formulate two equations with these two quantities as unknowns for simultaneous solution. This can be done by examining the aircraft equations of motion in conjunction with the equations for aircraft lift and moment.

The sum of the forces in the direction perpendicular to the free stream velocity can be expressed by

$$m a_n = L - mg \cos \gamma_d + T_e \sin(\epsilon + \alpha_r) \quad (104)$$

where a_n is normal acceleration, L is lift, T_e is the thrust estimate (this quantity will be approximated by the thrust required from the previous instant), and ϵ is the thrust line offset. Using a small angle approximation for the sine term simplifies the equation and is a valid assumption provided the angle of attack and thrust line offset are small. For a "hard" ride during the terrain following task, the optimal spline path is restricted to -1 "g" and plus 2 "g" from nominal (Ref 11). With this restriction, the angle of attack is limited to a small angle validating the assumption.

The lift term can be expressed by

$$L = C_L \bar{q} S \quad (105)$$

where C_L is the total lift coefficient, \bar{q} is the dynamic pressure, and S is the total surface area. In addition

$$C_L = C_{L_0} + C_{L_\alpha} \alpha + C_{L_{\delta e}} \delta e + C_{L_q} \frac{\bar{c} q_r}{2 V} \quad (106)$$

where C_{L_0} is the total aircraft lift coefficient for $\alpha = \delta e = 0$, C_{L_α} is the total aircraft lift curve slope, $C_{L_{\delta e}}$ is

the change in total lift coefficient for a unit elevator angle, C_{L_q} is the change in lift coefficient for a change in pitch rate, \bar{c} is the mean aerodynamic chord length, and q_r is the reference pitch rate. For the problem under consideration, C_{L_0} equals zero. Also, since

$$q_r = \dot{\alpha}_r + \dot{\gamma} \quad (107)$$

$$\text{then } C_L = C_{L_\alpha} \alpha_r + C_{L_{\delta e}} \delta e_r + C_{L_q} \frac{\bar{c}(\dot{\alpha}_r + \dot{\gamma})}{2 V} \quad (108)$$

The normal acceleration can be expressed in terms of curvature by

$$a_n = V^2 K \quad (109)$$

Substituting the above relationships into equation (104) and rearranging terms results in the following

$$\begin{aligned} (C_L + \frac{T_e}{\bar{q}S}) \alpha_r + C_{L_{\delta e}} \delta e_r &= \frac{(mV^2 K + mg \cos \gamma - T_e \epsilon)}{\bar{q}S} \\ &+ \frac{C_{L_q} \bar{c} (\dot{\alpha}_r + \dot{\gamma})}{2 V} \end{aligned} \quad (110)$$

It is now necessary to estimate the reference angle of attack and its derivatives. This estimated angle of attack, α_e , will not be used explicitly in the reference command generator, but it is necessary in order to obtain the derivative of the angle of attack for use in equation (110). This estimate of the angle of attack derivative will also be used to calculate the reference pitch rate as indicated in the next section.

In order to arrive at an estimate, it will be assumed that

$$C_L \approx C_{L_\alpha} \alpha_e \quad (111)$$

then

$$\alpha_e = \frac{m(V^2 K + g \cos \gamma)}{(\bar{q} S C_{L_\alpha} + T_e)} \quad (112)$$

Letting

$$C_A = \frac{m}{(\bar{q} S C_{L_\alpha} + T_e)} \quad (113)$$

and

$$V_{dg} = V^2 K + g \cos \gamma \quad (114)$$

the estimated angle of attack becomes

$$\alpha_e = C_A V_{dg} \quad (115)$$

And the derivative of the estimated angle of attack is

$$\dot{\alpha}_e = \dot{C}_A V_{dg} + C_A \dot{V}_{dg} \quad (116)$$

or

$$\dot{\alpha}_e = (\dot{C}_A / C_A) \alpha_e + C_A \dot{V}_{dg} \quad (117)$$

where

$$\dot{C}_A = \frac{-C_A^2 (\dot{\bar{q}} S C_{L_\alpha} + \dot{T}_e)}{m} \quad (118)$$

and

$$\dot{V}_{dg} = 3 V \dot{V} K + K V^2 \quad (119)$$

The second derivatives of equations (117), (118), and (119) are required for use in the forthcoming moment equation and can be evaluated as

$$\ddot{\alpha}_e = \ddot{C}_A V_{dg} + 2 \dot{C}_A \dot{V}_{dg} + C_A \ddot{V}_{dg} \quad (120)$$

with

$$\ddot{C}_A = \frac{-2 C_A \dot{C}_A (\dot{\bar{q}} S C_{L_\alpha} + \dot{T}_e)}{m} - \frac{C_A^2 (\ddot{\bar{q}} S C_{L_\alpha} + \ddot{T}_e)}{m} \quad (121)$$

$$\text{And } \ddot{V}_{dg} = 3 \dot{V}^2 K + 3 V \ddot{V} K + 5 V \dot{V} \dot{K} + V^2 \ddot{K} \quad (122)$$

where the dynamic pressure is

$$\bar{q} = \frac{1}{2} \rho V^2 \quad (123)$$

and its derivatives are

$$\dot{\bar{q}} = \rho \dot{V} V \quad (124)$$

$$\ddot{\bar{q}} = \rho (\ddot{V} V + \dot{V}^2) \quad (125)$$

where air density, ρ , is assumed constant. The estimated thrust derivatives \dot{T}_e and \ddot{T}_e will be approximated by first backward difference equations. The expression for \dot{K} is shown in equation (102). The second derivative is

$$\begin{aligned} \ddot{K} = & \frac{\dot{V} \dot{K}}{V} + V^2 (\cancel{h''''} \cos^5 \gamma - 4h'''' h' K \cos^4 \gamma \\ & - \frac{6 K \dot{K} h'}{V} - 3K^2 h'' \cos \gamma) \end{aligned} \quad (126)$$

For the cubic spline the fourth derivative, h'''' , will be approximated by zero.

Using the basic relationship of equation (108), there still remains the two unknowns α_r and δe_r . This requires an examination of the moment equation in order to have two equations and two unknowns. The moment equation can be expressed by

$$I_{yy} \dot{q} = M_A + \cancel{M_T} \quad (127)$$

where I_{yy} is the moment of inertia about the y-axis, M_A is the moment due to the aerodynamic forces, and M_T is the moment due to thrust. M_T for the aircraft under study is zero. Thus, the total moment is equal to the moment due to the aerodynamic forces. Expanding the right side of the equation yields

$$M_A = C_M \bar{q} S \bar{c} \quad (128)$$

where C_M is the total aircraft pitching moment coefficient. This coefficient can be expressed as

$$C_M = C_{M_\alpha} \alpha_r + C_{M_{\delta e}} \delta e_r + C_{M_q} \frac{\bar{c} q_r}{2V} \quad (129)$$

where C_{M_α} is the total aircraft pitching moment coefficient versus angle of attack slope, $C_{M_{\delta e}}$ is the change in total aircraft pitching moment coefficient for a unit elevator angle, and C_{M_q} is the change in the moment coefficient for unit change in pitch rate.

$$\text{Since } q_r = \dot{\alpha}_e + \dot{\gamma} \quad (130)$$

$$\text{then } \dot{q}_r = \ddot{\alpha}_e + \ddot{\gamma} \quad (131)$$

Substituting the above equations into equation (127) and rearranging terms, the moment equation becomes

$$C_{M_\alpha} \alpha_r + C_{M_{\delta e}} \delta e_r = \frac{I_{yy}(\ddot{\alpha}_e + \ddot{\gamma})}{\bar{q} S \bar{c}} - \frac{C_{M_q}(\dot{\alpha}_e + \dot{\gamma})\bar{c}}{2V} \quad (132)$$

In order to simplify the required manipulations, the following quantities are defined

$$C_{L_{\alpha}}^* \equiv C_{L_{\alpha}} + \frac{T_e}{\bar{q} S} \quad (133)$$

$$\Delta C_{L_d} \equiv \frac{(mV^2 K + mg \cos \gamma - T_e \epsilon)}{\bar{q} S} + \frac{C_{Lq} \bar{c} (\dot{\alpha}_e + \dot{\gamma})}{2 V} \quad (134)$$

$$\Delta C_{M_d} \equiv \frac{I_{yy} (\ddot{\alpha}_e + \ddot{\gamma})}{\bar{q} S \bar{c}} - \frac{C_{Mq} (\dot{\alpha}_e + \dot{\gamma}) \bar{c}}{2 V} \quad (135)$$

The lift equation (equation (110)) and the moment equation (equation (132)) can be expressed in matrix form as

$$\begin{bmatrix} C_{L_{\alpha}}^* & C_{L_{\delta e}} \\ C_{M_{\alpha}} & C_{M_{\delta e}} \end{bmatrix} \begin{bmatrix} \alpha_r \\ \delta e_r \end{bmatrix} = \begin{bmatrix} \Delta C_{L_d} \\ \Delta C_{M_d} \end{bmatrix} \quad (136)$$

The leading matrix is non-singular; thus

$$\begin{bmatrix} \alpha_r \\ \delta e_r \end{bmatrix} = \frac{1}{C_{L_{\alpha}}^* C_{M_{\delta e}} - C_{M_{\alpha}} C_{L_{\delta e}}} \begin{bmatrix} C_{M_{\delta e}} & -C_{L_{\delta e}} \\ -C_{M_{\alpha}} & C_{L_{\alpha}}^* \end{bmatrix} \begin{bmatrix} \Delta C_{L_d} \\ \Delta C_{M_d} \end{bmatrix} \quad (137)$$

Solving for α_r and δe_r yields

$$\alpha_r = \frac{C_{M_{\delta e}} \Delta C_{L_d} - C_{L_{\delta e}} \Delta C_{M_d}}{C_{L_{\alpha}}^* C_{M_{\delta e}} - C_{M_{\alpha}} C_{L_{\delta e}}} \quad (138)$$

$$\delta e_r = \frac{C_{L_{\alpha}}^* \Delta C_{M_d} - C_{M_{\alpha}} \Delta C_{L_d}}{C_{L_{\alpha}}^* C_{M_{\delta e}} - C_{M_{\alpha}} C_{L_{\delta e}}} \quad (139)$$

Now that the reference angle of attack has been established, it is possible to update the estimated first derivative of the angle of attack, $\dot{\alpha}_e$, for use in defining the pitch rate ref-

erence, q_r .

Reference Pitch Rate. In order to increase the accuracy of the reference pitch rate, a first order Taylor series expansion is accomplished for the estimated first derivative of the angle of attack. This updated derivative is then summed with the first derivative of the flight path angle to form the reference pitch rate.

A first order Taylor series expansion of $\dot{\alpha}$ results in

$$\dot{\alpha}_r = \dot{\alpha}_e + \frac{\partial \dot{\alpha}_e}{\partial \alpha} \Delta \alpha \quad (140)$$

Using $\dot{\alpha}_e$ as defined in equation (117), the expansion becomes

$$\dot{\alpha}_r = \dot{\alpha}_e - \frac{C_A(\dot{q} S C_{L_\alpha} + \dot{T}_e)(\alpha_r - \alpha_e)}{m} \quad (141)$$

The updated reference pitch rate is

$$q_r = \dot{\alpha}_r + \dot{\gamma} \quad (142)$$

Reference Thrust Command. The reference thrust command can be calculated from the drag equation.

$$m\dot{V} = T_r \cos(\alpha_r + \epsilon) - D - mg \sin \gamma \quad (143)$$

where D is the total drag and T_r is the reference thrust.

From equation (92)

$$\dot{V} = -g \sin \gamma \quad (144)$$

Thus, the reference thrust is

$$T_r = \frac{D}{\cos(\alpha_r + \epsilon)} \quad (145)$$

Drag can be expressed by

$$D = \bar{q} S C_D \quad (146)$$

The total drag coefficient, C_D , can be approximated by

$$C_D \approx C_{D_0} + \frac{C_L^2}{\pi A e} \quad (147)$$

where C_L is the total aircraft lift coefficient, C_{D_0} is the aircraft drag coefficient at $C_L = 0$, A is the aspect ratio, and e is the efficiency factor. Since the reference pitch rate has been determined, the coefficient of lift can be evaluated using equation (106). Thus, the reference thrust command can be obtained through the solution of equations (145), (146), and (147).

Reference State and Control Vectors. Utilizing the values obtained thus far for the reference angle of attack, the first derivative of the angle of attack, the reference thrust command, the first derivative of the flight path angle, and the flight path angle, the reference state vector becomes

$$\underline{x}_r = \begin{bmatrix} u_r \\ w_r \\ q_r \\ \theta_r \\ \delta e_r \\ T_r \\ h_r \end{bmatrix} = \begin{bmatrix} V_d \cos \alpha_r \\ V_d \sin \alpha_r \\ \dot{\alpha}_r + \gamma_d \\ \alpha_r + \gamma_d \\ \delta e_r \\ T_r \\ h_d \end{bmatrix} \quad (148)$$

The control vector is composed of the elevator and thrust

reference states

$$\underline{u}_r = \begin{bmatrix} \delta e_r \\ T_r \end{bmatrix} \quad (149)$$

The proposed system can now be implemented as described in Chapter I.

Hybrid Simulation of the Terrain Following Task.

The terrain following task was simulated on a Xerox Sigma 7, 32 bit, 112K hybrid computer with 15 bit plus sign analog to digital and digital to analog converters. The command follower system as shown in Figure 1 of Chapter I was implemented on the hybrid computer using the reference command generator developed previously in this chapter, the non-linear aircraft model developed in Appendix A, and the discrete optimal feedback gain matrix, \underline{K} , based on the performance index developed in Chapter III. A short segment of terrain (50,000 feet) was used in the simulation from which a 100 foot clearance path and optimal cubic spline path were generated (Ref 11). The sample terrain and associated paths are shown in Figure 30. The desired altitude and slope at 1000 foot discrete horizontal range increments were stored for optimal path reconstruction by the REFCOM program. The desired path was constrained to remain within a minus one to a plus two "g" normal acceleration boundary. The system was observed at sample rates from 100 hertz down to 2 hertz (twice the Nyquist rate). The state response of the system for 100, 5, and 2 hertz sample rates is shown in Figures 31 through 38.

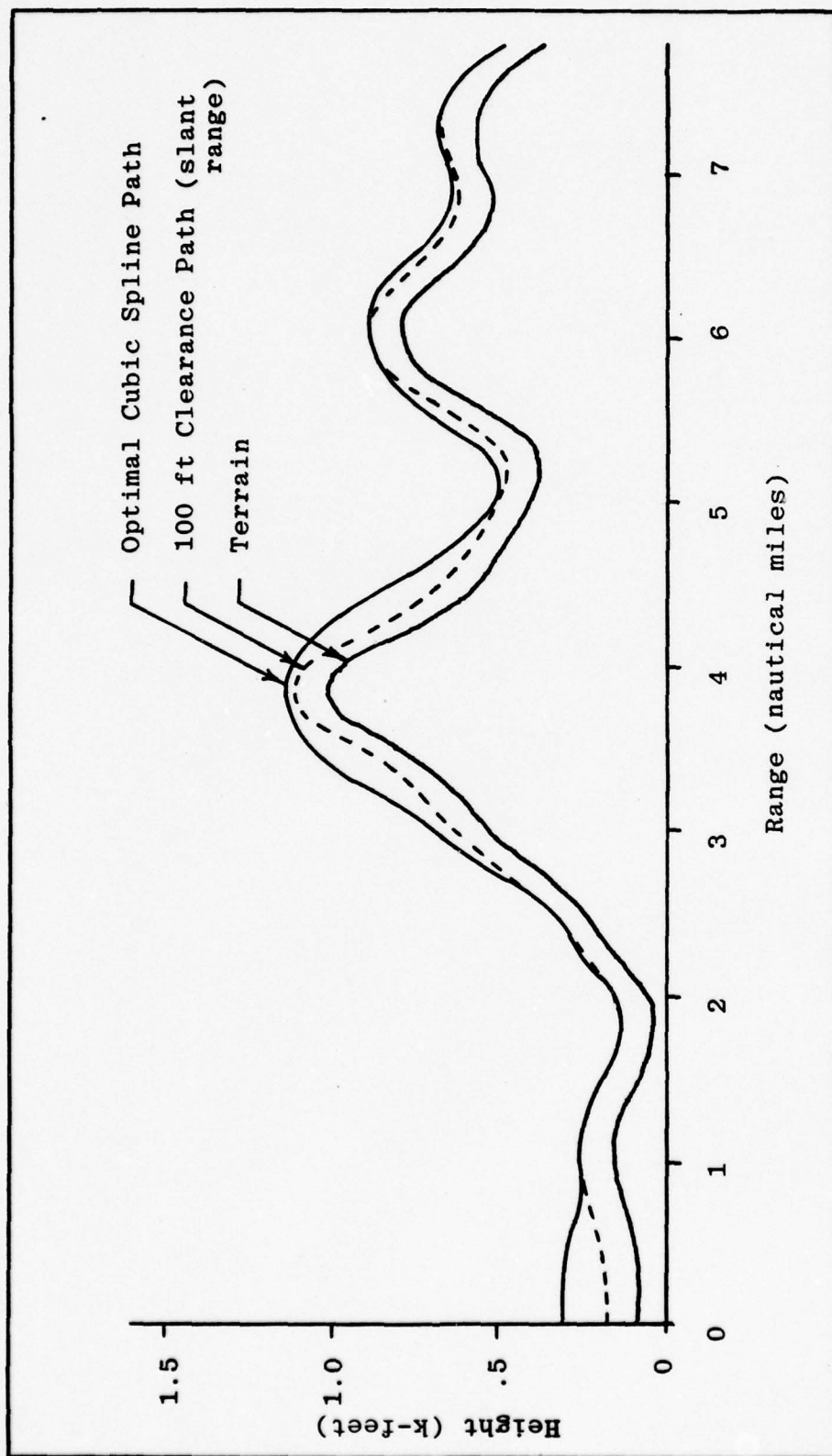


Figure 30. Optimal cubic spline path and terrain for hybrid simulation.

The error vector quantities (state minus reference vector) are shown in Figures 39 through 45.

As shown in the associated figures, the state response is nearly identical for sample rates from 100 to 5 hertz. The primary difference is in the response of the elevator state as indicated in Figure 35. A greater maximum and minimum deflection is required at the five hertz sample rate. It is interesting to note the state behavior at a sample rate of two hertz. Only slight degradation of the state response can be observed. In fact, the elevator response has been smoothed at this low sample rate.

Of further interest is the relationship shown when the thrust time history, Figure 36, is compared to the angle of attack history, Figure 37. Since the reference command generator was based on a simplified constant energy control, as angle of attack is increased depleting the energy level through aircraft "g" loading a resulting thrust command is required to restore the depleted energy. To further reduce thrust fluctuation, in order to achieve less engine cycling and wear, it would be necessary to incorporate a means of allowing the energy level to vary between a lower and upper limit. This could be implemented through software changes quite readily.

Even though the altitude response as shown in Figure 38 is remarkably similar for a wide range of sample rates, it is necessary to examine the error between actual and reference altitude to determine acceptability. This error is illustrated in Figure 39. The maximum absolute error is 13 feet

at 100 hertz and increases to 22 feet at a five hertz sample rate. For a two hertz rate, the absolute error increases to 34 feet. Thus, the five hertz sample rate could be deemed to be quite acceptable in this tracking task, while the two hertz system could be deemed as inadequate. This is also verified by the other state variable responses at the two hertz sample rate. If it were required to guarantee a minimum clearance path altitude, the optimal path altitude could be shifted upward by the maximum error to insure achievement of the desired clearance minimum. It is also entirely possible to decrease the error quantity by tuning of the controller.

The other error states are included in Figure 40 through 45 for the interested reader.

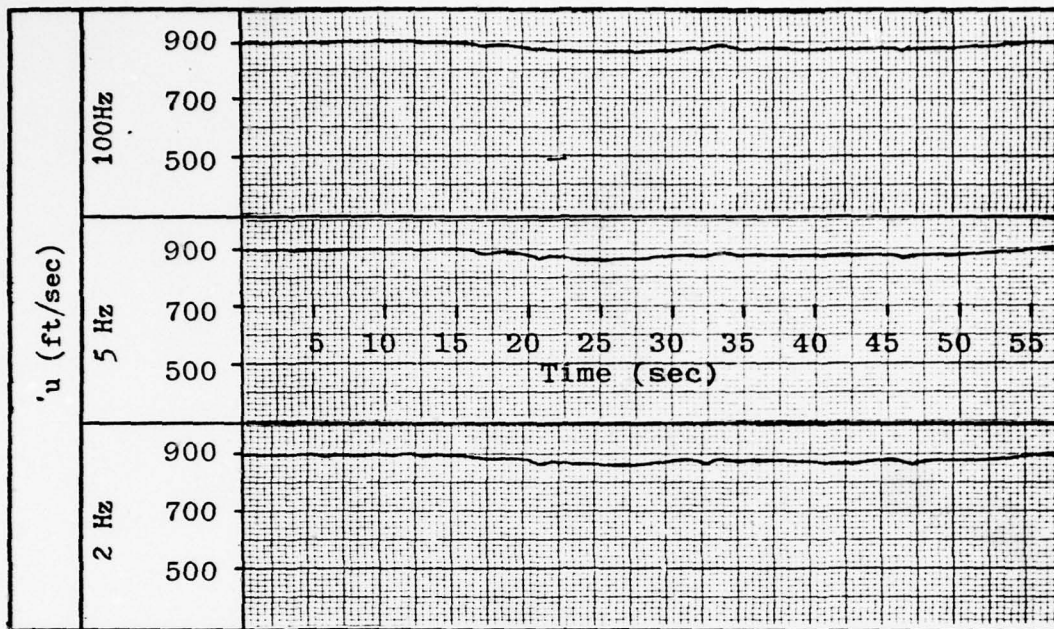


Figure 31. Longitudinal velocity, u , as a function of time.

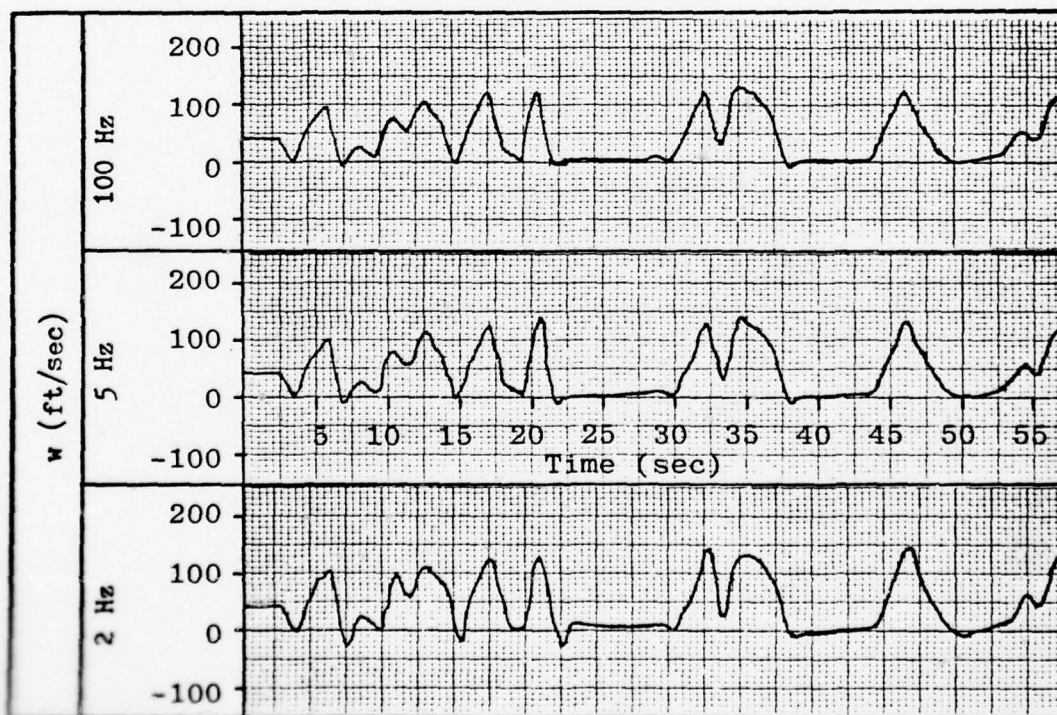


Figure 32. Vertical velocity, w , as a function of time.

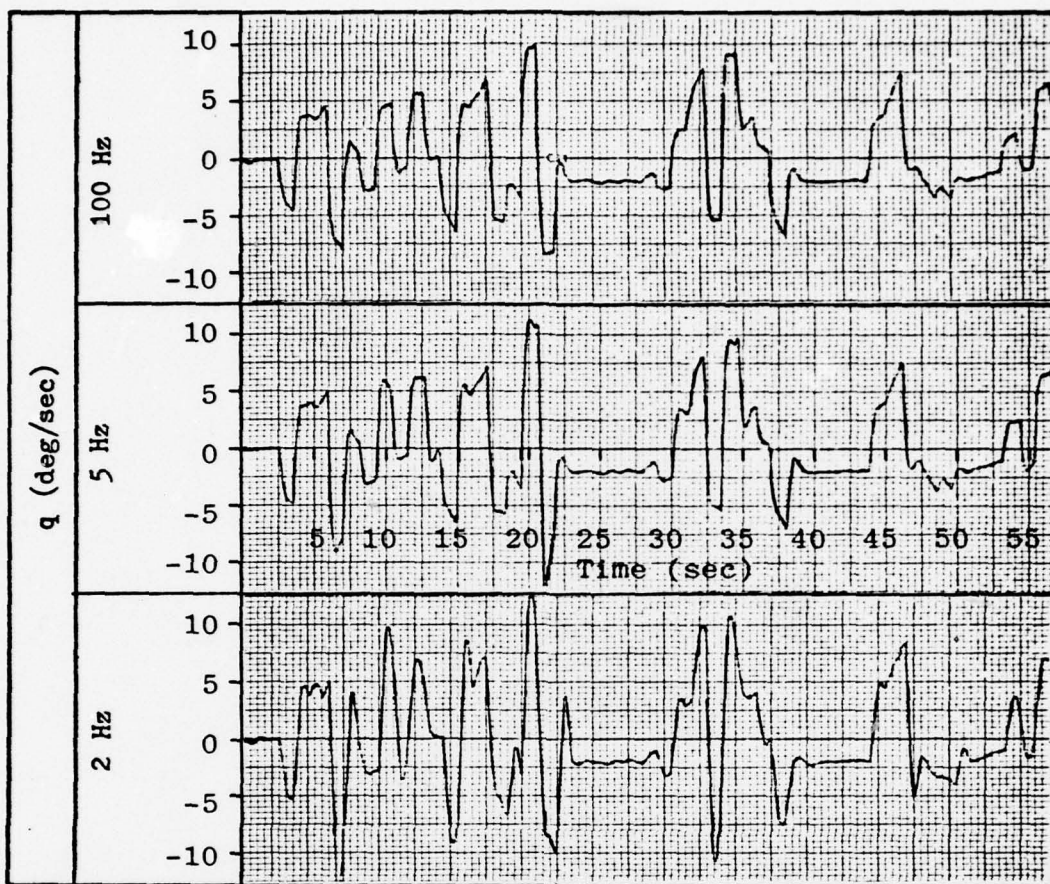


Figure 33. Pitch rate, q , as a function of time.

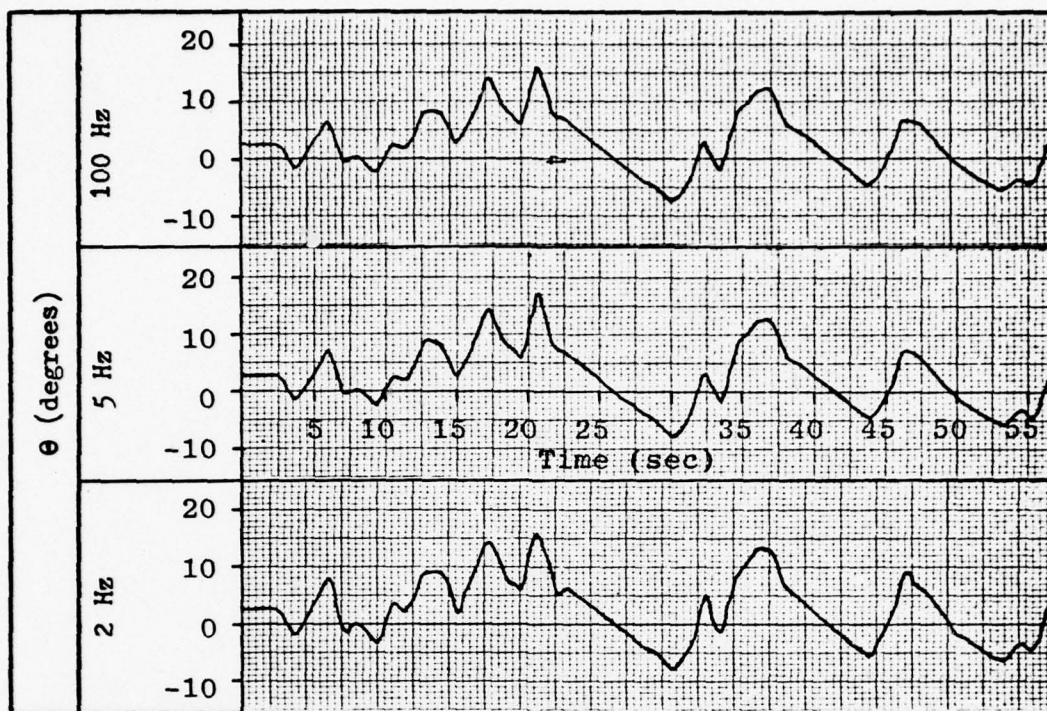


Figure 34. Pitch angle, θ , as a function of time.

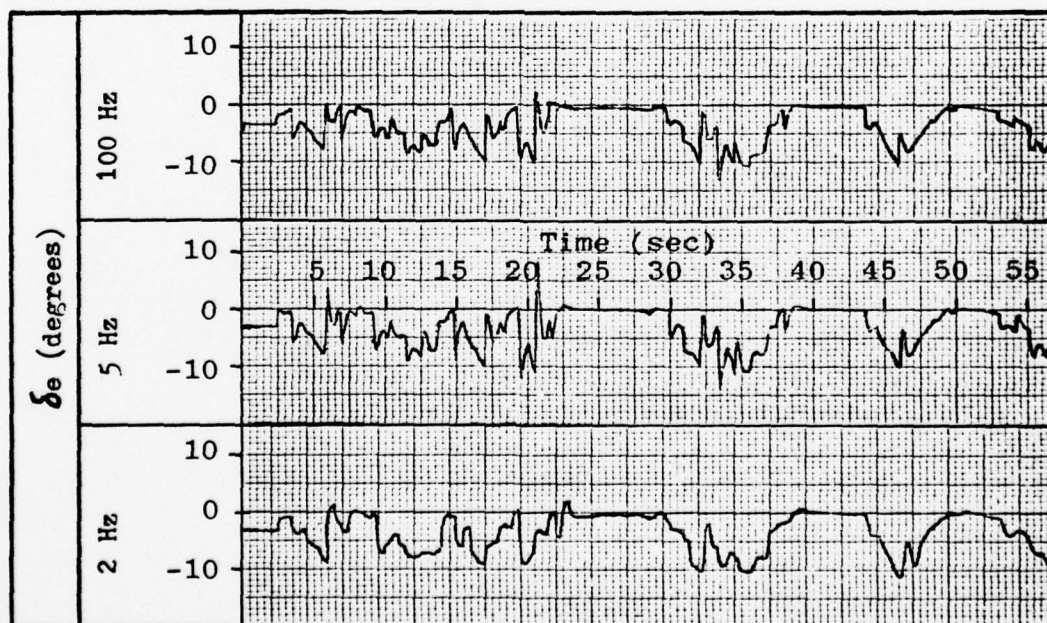


Figure 35. Elevator angle, δ_e , as a function of time.

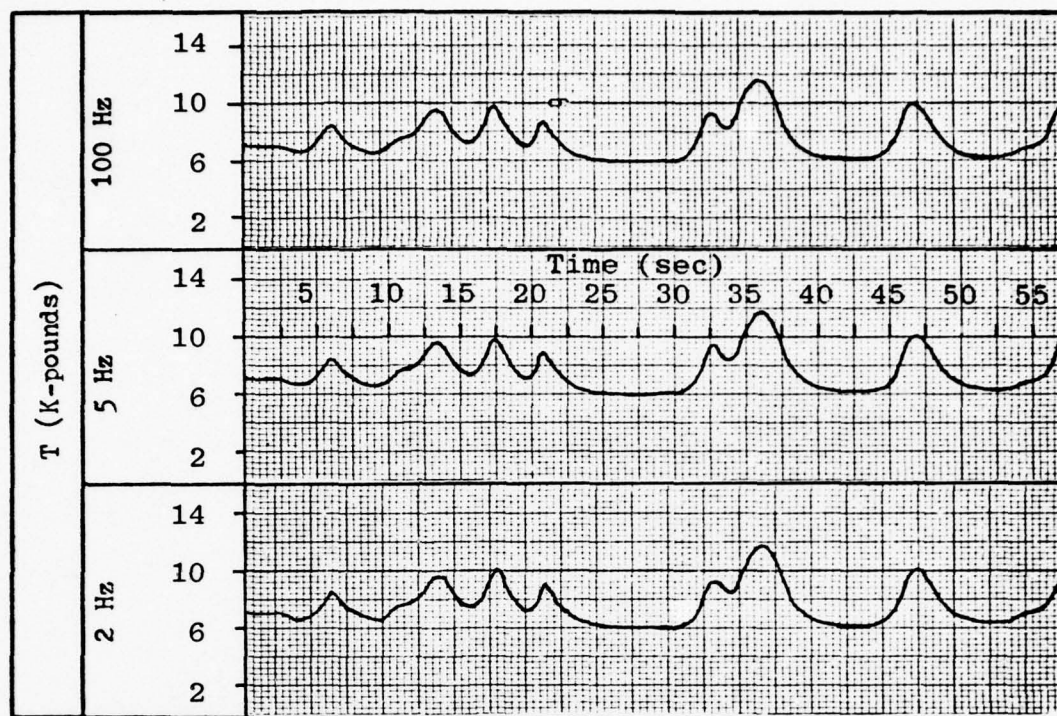


Figure 36. Thrust, T , as a function of time.

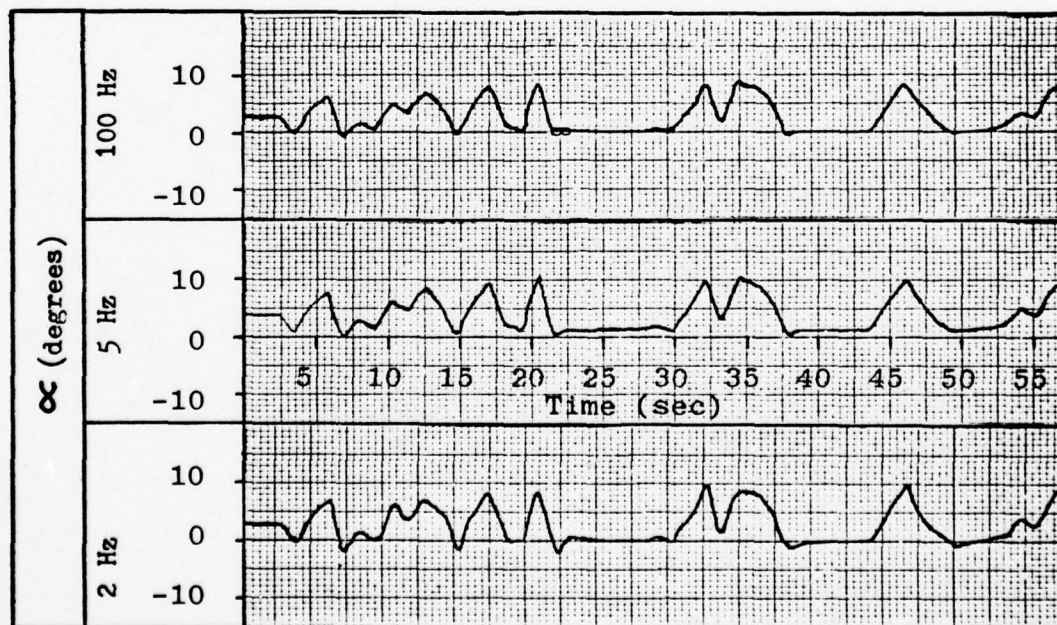


Figure 37. Angle of attack, α , as a function of time.

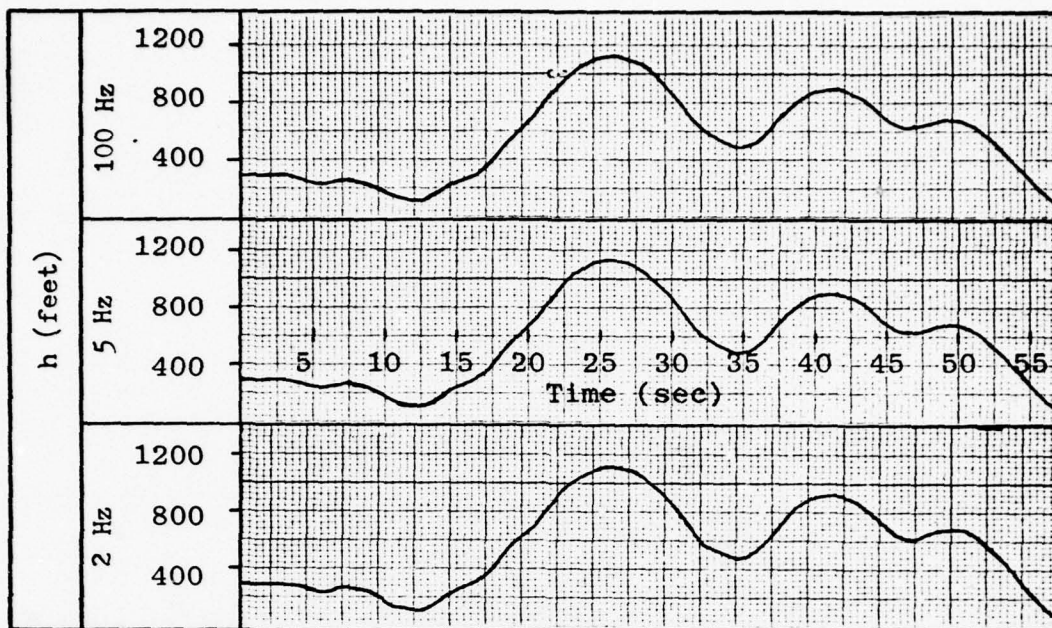


Figure 38. Altitude, h , as a function of time.

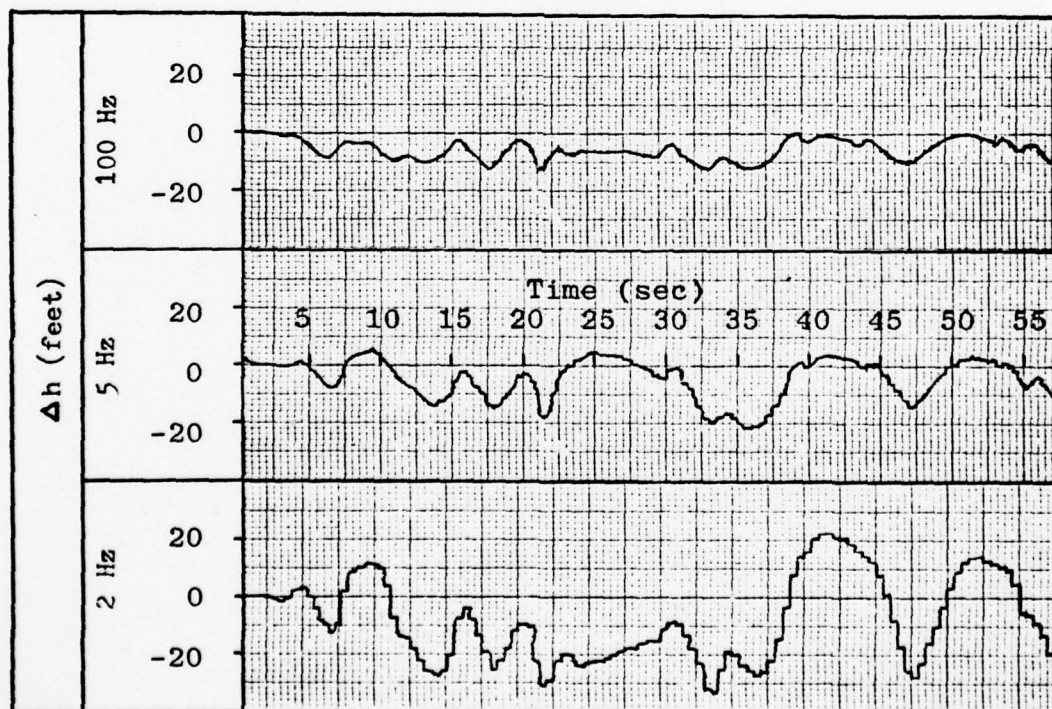


Figure 39. Error in altitude, Δh , between actual and reference.

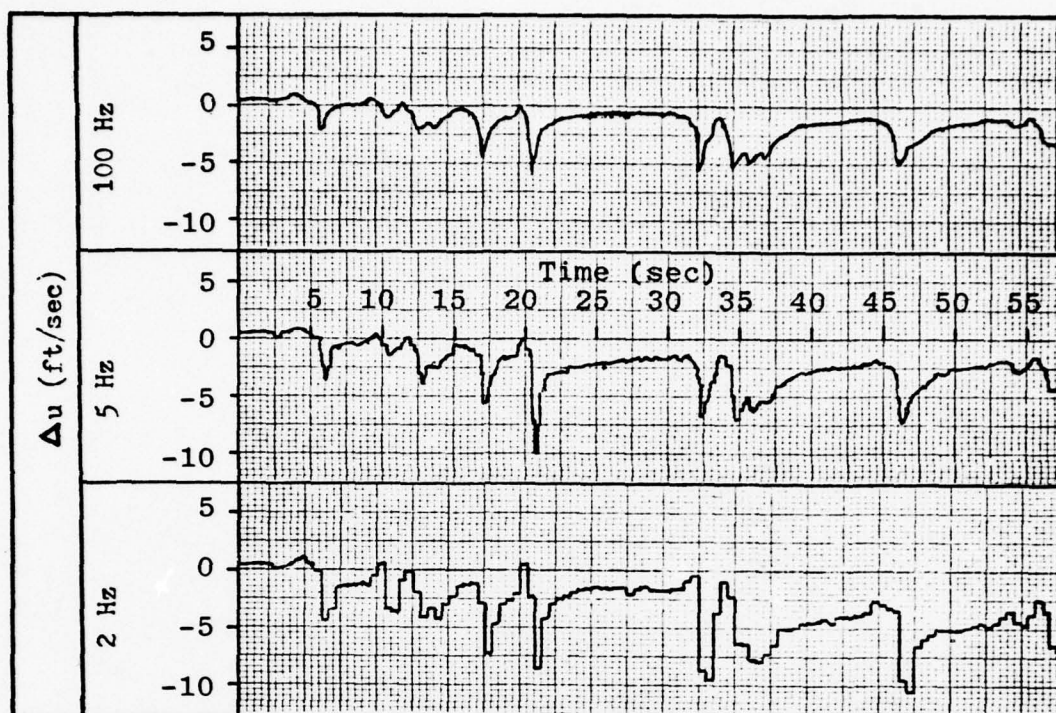


Figure 40. Error in longitudinal velocity, Δu , between actual and reference.

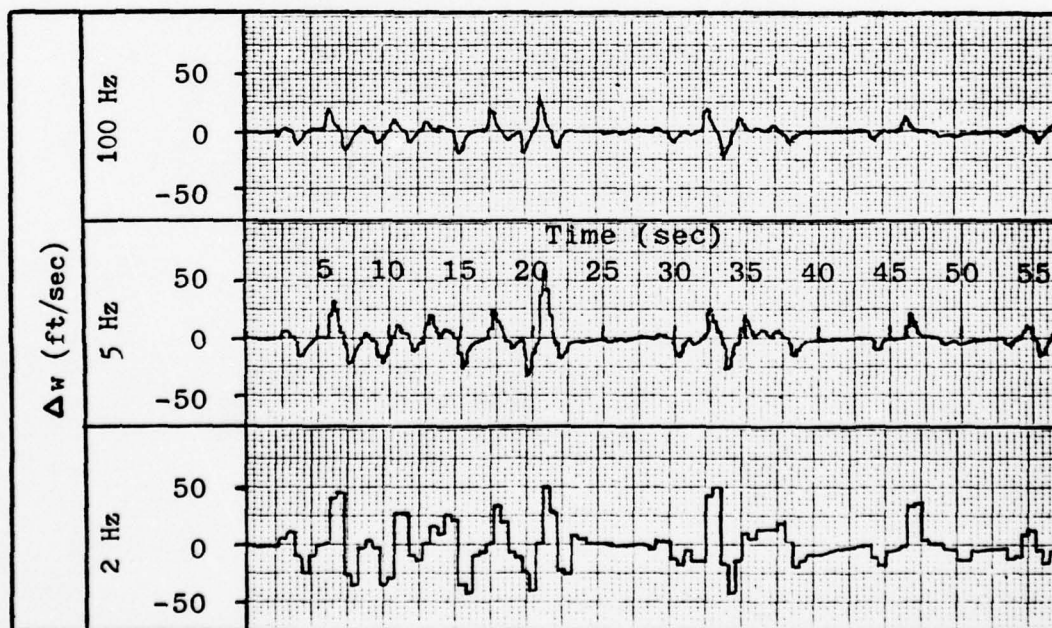


Figure 41. Error in vertical velocity, Δw , between actual and reference.

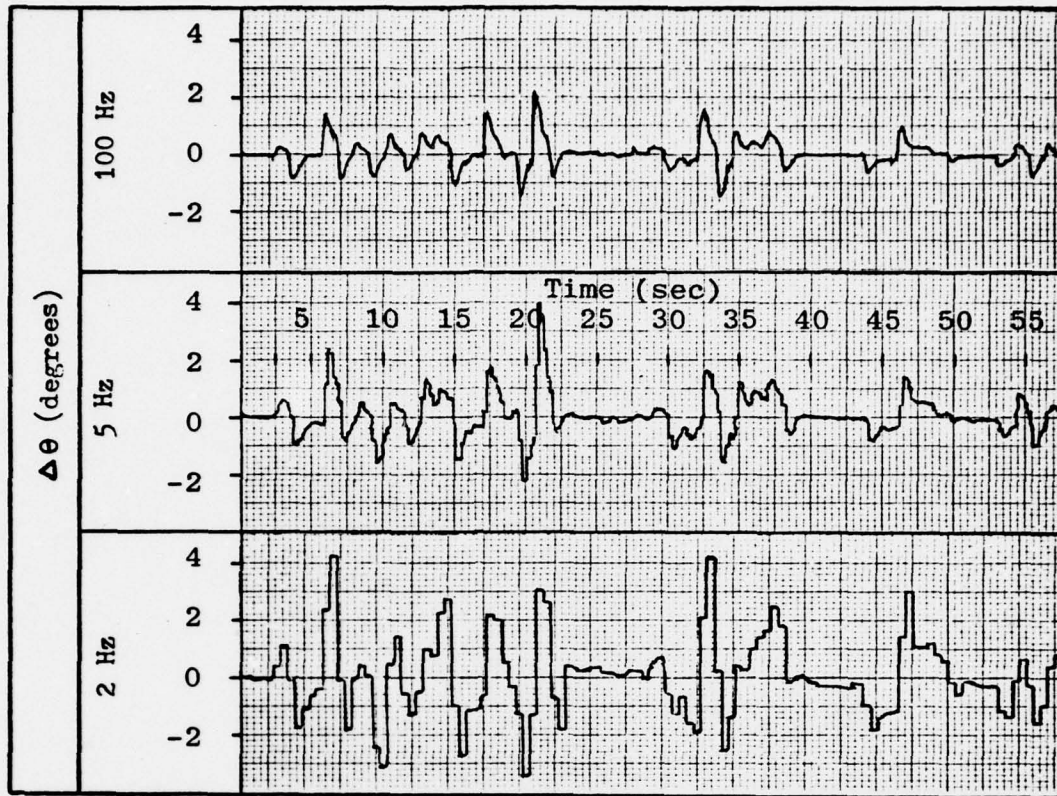


Figure 42. Error in pitch angle, $\Delta\theta$, between actual and reference.

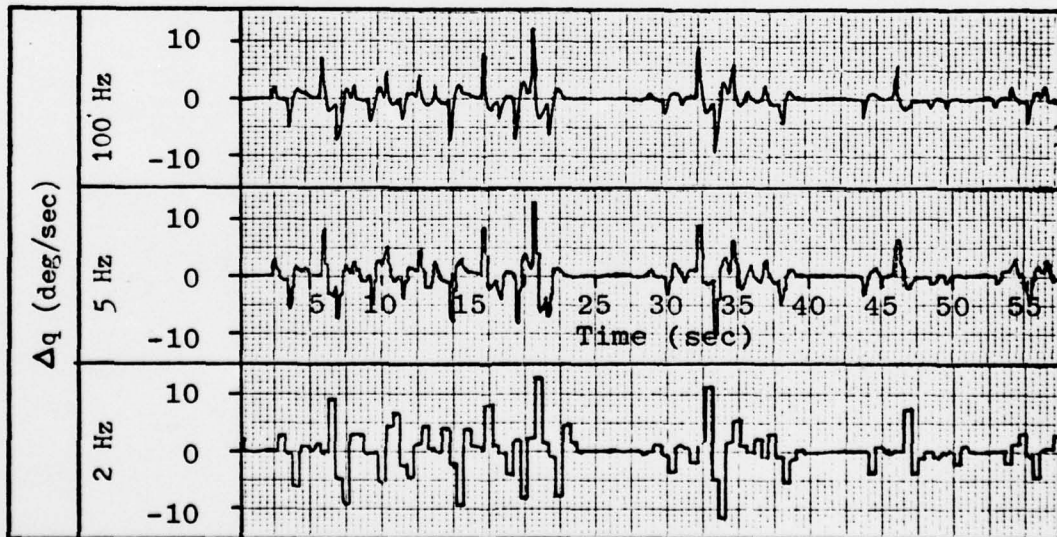


Figure 43. Error in pitch rate, Δq , between actual and reference.

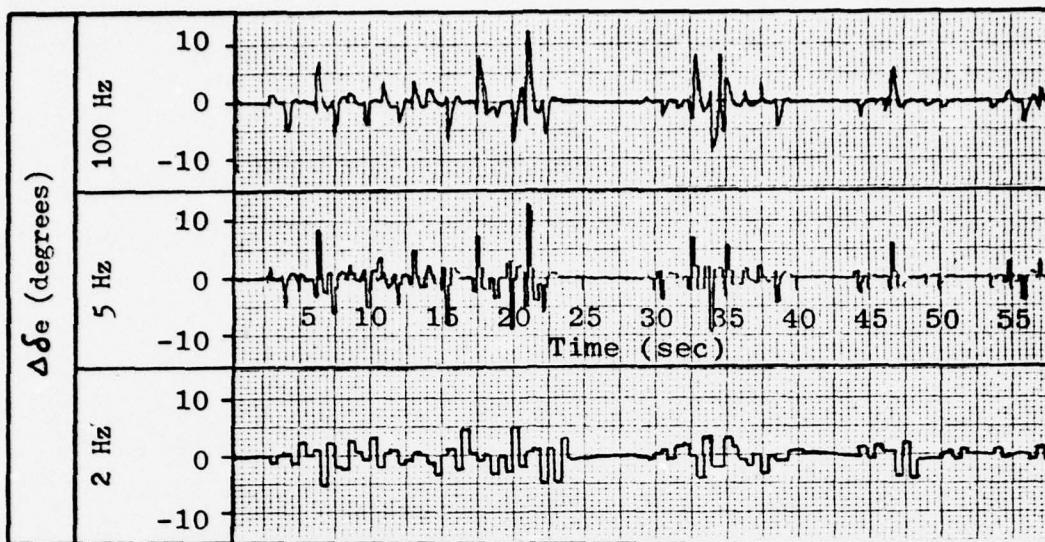


Figure 44. Error in elevator deflection angle, $\Delta\delta_e$, between actual and reference.

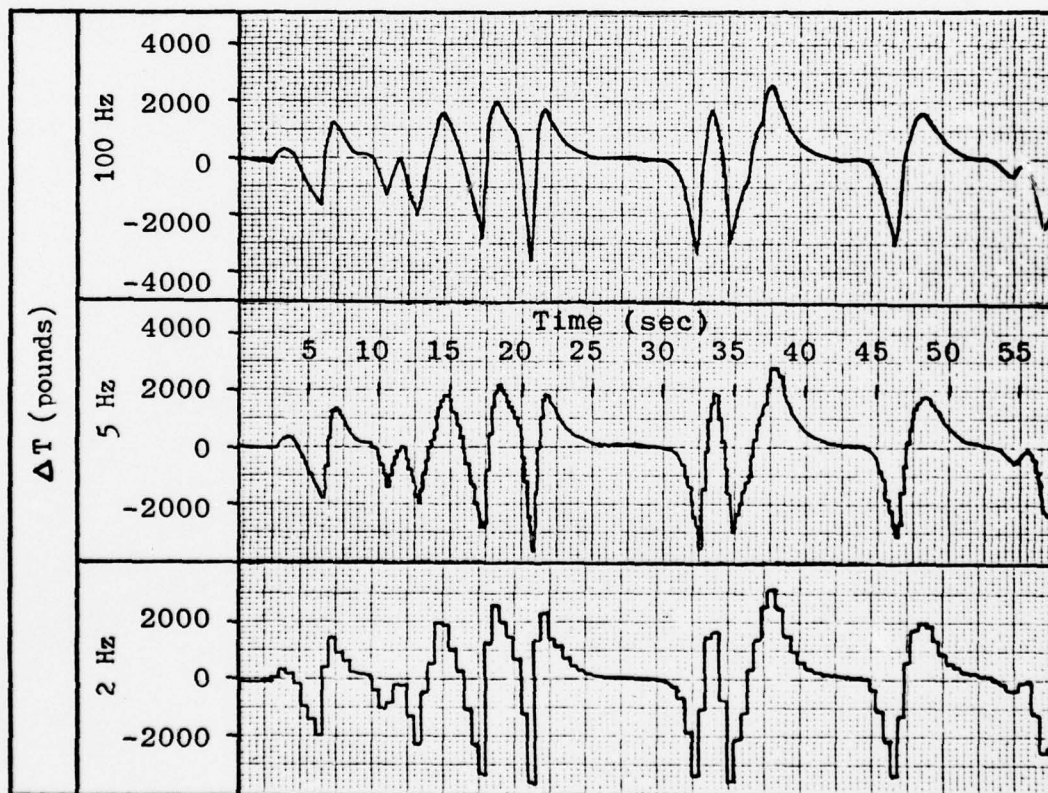


Figure 45. Error in thrust setting, ΔT , between actual and reference.

VI. Conclusions and Recommendations

Conclusions

The breakthroughs of the recent past have provided the control engineer with a new method for the implementation of an aircraft flight control system. Through the use of state space, continuous optimal control, and discrete optimal control, a digital flight control system has been designed for the terrain following task. After formulating the aircraft linear perturbation model, the deterministic regulator problem was solved iteratively to provide the state cost and control cost matrices for the desired continuous closed loop system. The selection of these matrices was based on the Cornell Aeronautical Laboratory "thumbprint" which specified the short period natural frequency and damping ratio. Once the matrices were selected, an analog computer simulation was accomplished to verify the "goodness" of the selection. As a side note, the controller was modified to yield a C^* response for comparison with C^* criteria. With the continuous cost matrices defined for the desired closed loop root location, the system was discretized, as was the continuous quadratic performance index, to form a discrete deterministic regulator problem.

The discrete regulator problem was solved as a function of sample rate to determine a minimum rate for sampling. This direct digital design technique has the advantage of not introducing errors into a discrete system analysis since the zero order hold is accounted for precisely. The effects

of sample rate on the system were then examined. The finite word length of a digital system was shown to produce the equivalent of a noise being introduced into the system. A sample rate of five hertz was shown to be high enough to adequately form the desired controls. A reference command generator was developed using as a basis a form of constant energy control. A hybrid simulation was then completed using a reference path generated by Funk's optimal cubic spline algorithm. The aircraft was shown to track the desired path in a highly acceptable manner.

Recommendations for Further Study

Since the system studied was assumed to be a perfect system with body bending and sensor noise not considered, it is recommended a stochastic study of the problem be conducted with these items taken into consideration. Also of interest would be the incorporation of an estimator or observer since for this study all states were assumed available. The noise due to finite word length could also be taken into account using a stochastic approach.

Another realm of interest would be an assessment of the required memory size for the control system. This study should include the requirements for the optimal cubic spline algorithm.

As a final recommendation, the approach taken in this study could be adopted for tasks other than terrain following. For instance, weapon delivery or air to air tracking would be of great interest.

Bibliography

1. Hartmann, G. L. and C. A. Harvey. "Digital Adaptive Control Laws for the F-8." American Institute of Aeronautics and Astronautics, 76-1952: 319-330 (August 1976).
2. A-7D Digital Multimode Flight Control System Flight Test and Weapon Delivery Evaluation. AFFDL-TR-76-121. Wright-Patterson Air Force Base, Ohio: Air Force Flight Dynamics Laboratory, December 1976.
3. Advanced Fighter Digital Flight Control System (DFCS) Definition Study. W0728-FR. Minneapolis, Minnesota: Honeywell, Inc., March 1975.
4. Powell, J. D., E. Parsons, and M. G. Tashker. Aircraft Digital Control Design Methods. SUDAAR 500. Stanford, California: Stanford University Guidance and Control Laboratory, Department of Aeronautics and Astronautics, February 1976.
5. Katz, P. and J. D. Powell. Selection of Sampling Rate for Digital Control of Aircrafts. SUDAAR 486. Stanford, California: Stanford University Guidance and Control Laboratory, Department of Aeronautics and Astronautics, September 1974.
6. Tobie, H. N., E. M. Elliott, and L. G. Malcom. A New Longitudinal Handling Qualities Criterion. Seattle, Washington: Commercial Airplane Division, The Boeing Company, 1965.
7. Roskam, J. Flight Dynamics of Rigid and Elastic Airplanes, Part 1. Kansas: Roskam Aviation and Engineering Corporation, 1976.
8. Funk, J. E. "Optimal-Path Precision Terrain Following System." American Institute of Aeronautics and Astronautics, 76-1958: 383-390 (August 1976).
9. Bryson, A. E. and W. E. Hall. Optimal Control and Filter Synthesis by Eigenvector Decomposition. SUDAAR 436. Stanford, California: Stanford University Department of Aeronautics and Astronautics, November 1971.
10. Kisslinger, R. L. and M. L. Wendl. Survivable Flight Control System Interim Report No. 1 Studies, Analysis and Approach. AFFDL-TR-71-20 Supplement 1. Wright-Patterson Air Force Base, Ohio: Air Force Flight Dynamics Laboratory, May 1971.
11. Funk, J. E. Terrain Following Control Based on an Optimized Spline Model of Aircraft Motion. ASD/XR-TR-75-22. Wright-

Bibliography (Continued)

Patterson Air Force Base, Ohio: Deputy for Development
Planning, Aeronautical Systems Division, November 1975.

Appendix A

Non-Linear Aircraft Model

For the problem under study, it is assumed that maneuvering is restricted to the longitudinal plane; thus, the longitudinal equations of motion become

$$m(\dot{U} + WQ) = -mg \sin \theta + F_{a_x} + F_{T_x} \quad (A-1)$$

$$m(\dot{W} - UQ) = mg \cos \theta + F_{a_z} + F_{T_z} \quad (A-2)$$

$$I_{yy}\dot{Q} = M_A + M_T \quad (A-3)$$

Further, for wings level non-turning flight

$$Q = \dot{\theta} \quad (A-4)$$

The approximations for the elevator and throttle actuators are

$$\dot{\delta e} = -10 \delta e + 10 \delta e_c \quad (A-5)$$

and

$$\dot{T} = -T + T_c \quad (A-6)$$

Altitude, h , can be defined by

$$h = V \sin \gamma \quad (A-7)$$

The force produced by thrust in the x-direction is

$$F_{T_x} = T \cos \epsilon \quad (A-8)$$

where ϵ is the angle the engine thrust line makes with the x-axis. In a similar fashion

$$F_{T_z} = -T \sin \epsilon \quad (A-9)$$

For the aircraft under study, ϵ is approximately 2.9 degrees. The thrust vector acts through the center of gravity; thus, the moment due to thrust is zero.

The aerodynamic forces acting in the x-direction can be expressed by

$$F_{a_x} = -D \cos \alpha + L \sin \alpha \quad (A-10)$$

the total drag is represented by

$$D = C_D \bar{q} S \quad (A-11)$$

where C_D is the total aircraft drag coefficient, S is the surface area, and \bar{q} is the dynamic pressure acting on the aircraft. Dynamic pressure can be evaluated by

$$\bar{q} = \frac{1}{2} \rho V^2 \quad (A-12)$$

where ρ is the atmospheric density and V is the total velocity. The total velocity is defined by

$$V^2 = U^2 + W^2 \quad (A-13)$$

The atmospheric density, ρ , is assumed constant over the realm of flight and is evaluated at sea level ($\rho_{sl} = .002377$ slugs/ft³). The total aircraft drag coefficient will be approximated by

$$C_D = C_{D_0} + \frac{C_L^2}{\pi A e} \quad (A-14)$$

where C_L is the total aircraft lift coefficient, C_{D_0} is the aircraft drag coefficient at $C_L = 0$, A is the aspect ratio, and e is the efficiency factor. It is further assumed that

AD-A055 196

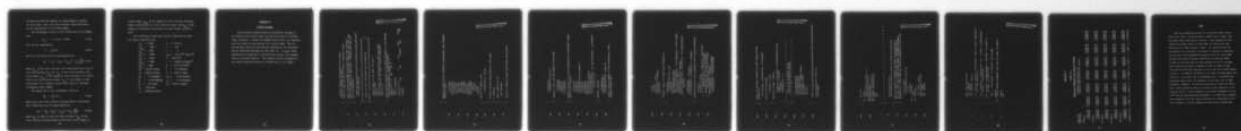
AIR FORCE INST OF TECH WRIGHT-PATTERSON AFB OHIO SCH--ETC F/G 1/3
THE TERRAIN FOLLOWING TASK FOR THE ADVANCED TACTICAL FIGHTER US--ETC(U)
DEC 77 R L SIMMONS
AFIT/6E/EE/77-39

UNCLASSIFIED

NL

2 OF 2

AD
A055196



END
DATE
FILMED
7-78
DDC

the Mach and Reynolds numbers are approximately constant for the flight; thus, the total aircraft drag coefficient can be approximated at this Mach number.

The aerodynamic forces in the z-direction can be summed into

$$F_{a_z} = -L \cos \alpha - D \sin \alpha \quad (A-15)$$

Lift can be expressed by

$$L = C_L \bar{q} S \quad (A-16)$$

The lift coefficient will be approximated by

$$C_L = C_{L_0} + C_{L_\alpha} \alpha + C_{L_{\delta e}} \delta e + C_{L_q} \frac{\bar{c} Q}{2 V} \quad (A-17)$$

Where C_{L_0} is the total aircraft lift coefficient for $\alpha = \delta e = 0$ (for this aircraft $C_{L_0} = 0$), C_{L_α} is the total aircraft lift-curve slope, $C_{L_{\delta e}}$ is the change in total aircraft lift coefficient for a unit elevator angle, C_{L_q} is the change in lift coefficient for a change in pitch rate, and \bar{c} is the mean aerodynamic chord length.

The moment due to the aerodynamic forces is

$$M_A = C_M \bar{q} S \bar{c} \quad (A-18)$$

where C_M is the total aircraft pitching moment coefficient.

This coefficient will be approximated by

$$C_M = C_{M_0} + C_{M_\alpha} \alpha + C_{M_{\delta e}} \delta e + C_{M_q} \frac{Q \bar{c}}{2 V} \quad (A-19)$$

where C_{M_0} is equal to zero for this aircraft, C_{M_α} is the total aircraft pitching moment coefficient versus angle of

attack slope, $C_{M_{\delta e}}$ is the change in total aircraft pitching moment coefficient for a unit elevator angle, and C_{M_q} is the change in the moment coefficient for unit change in pitch rate.

The coefficient values and initial conditions for the non-linear simulation are

C_{L_α}	= 2.066	\bar{c}	= 18.6 ft
$C_{L_{\delta e}}$	= .1383	A	= 2.5
C_{L_q}	= -.542	e	= .9
C_{D_0}	= .0106	I_{yy}	= $.38 \times 10^6$ slug ft ²
C_{M_α}	= -.1833	S	= 647 ft ²
$C_{M_{\delta e}}$	= -.1529	ρ	= .002377 slugs/ft ³
C_{M_q}	= -.651	g	= 32.174 ft/sec ²
W_0	= 42.65 ft/sec	ϵ	= 2.9 degrees
V_0	= 882.0 ft/sec	m	= 1709.4 slugs
Q_0	= 0.0 deg/sec	δe_0	= - 3.324 degrees
θ_0	= 2.772 degrees	α_0	= 2.772 degrees
R_0	= 0.0 feet	T_0	= 7091.2 pounds
H_0	= 300 feet		
U_0	= 880.96 ft/sec		

Appendix B

REFCOM Program

The following program requires precomputed storage of the desired cubic spline path altitude and slope at discrete range intervals. Subroutine PATHGEN reconstructs the required path and forms its derivatives for a given range. The required path slope and altitude was provided by the optimized spline algorithm developed by Funk (Ref 11). Certain other parameters are required to interactively operate the program from an intercom terminal. The complete digital program for the hybrid simulation was not included due to its length.

```

1  PROGRAM REFCOM(I INPUT,OUTPUT, TAPE7,TAPE8)
   *  REFERENCE COMMAND GENERATOR
   *  ARRAY XD WILL CONTAIN THE DESIRED REFERENCE STATES
   *
5  NEED TO READ IN NUMBER OF SPLINE POINTS (NSP) DEFINING
   *  LENGTH OF RUN ON FIRST DATA CARD.  ARRAY RI, ALT, SI, AND
   *  TER EITHER READ IN OR FROM TAPE7.  TERRAIN (TER) WILL BE
   *  USED FOR PLOTTING.
   *
10 COMMON RI(200),ALT(200),SI(200),NSP,RG,H,HI,HII,HIII,XD(7)
   *  DIMENSION TER(200)
   *
   * *****
   *  PRINT AND READ STATEMENTS FOR INTERCOM USE
   *  *
   * *****
   *
20 PRINT*, "WHAT IS THE VALUE FOR NSP? "
   *  READ 200,NSP
   *  PRINT*
   *  READ(7,300) (RI(I),ALT(I),SI(I),TER(I),I=1,NSP)
   *  PRINT*, "WHAT IS THE RANGE INCREMENT DESIRED? "
   *  READ*,XINC
   *
25 HO IS ENERGY ALTITUDE, VO IS ENERGY VELOCITY, TR IS INITIAL
   *  CONDITION ON THRUST, T IS SAMPLE PERIOD.
   *  PRINT*, "WHAT ARE THE VALUES FOR : "
   *  PRINT*, " T T 40 VO "
   *  PRINT*
   *  READ*,T,TE,HO,VO
   *
30 PRINT(8,*) " RG
   *  UP
   *  RG=XINC
   *
   *  H HI THETAR DER HIII
   *  TR"
35

```


THIS PAGE IS BEST QUALITY PRACTICABLE
FROM COPY FURNISHED TO DDC

REQUIRED COEFFICIENTS, STABILITY DERIVATIVES, AND AIRCRAFT
SPECIFICATIONS

GE=32.174
RHO=.002377
XMASS=1709.43
CLA=2.066
CLIF=.1383
CLO=-.542
CNO=.0106
CMA=-.1833
CMFE=-.1529
CMO=-.651
CBAR=13.6
PIASF=7.06853
XIVY=.38E06
S=647.
E=.0506
TR=TE
TE10P=0.

CALCULATE ENERGY LEVEL

$$EO = (VO^{*}2) / 2 . + GE^{*}HO$$

PROGRAM REPEATS CALCULATION AT THIS POINT

5 CONTINUE

RANGE LOOK UP BY AOC

CALL PATHGEN

CALCULATE DESIRED FLIGHT PATH ANGLE AND VELOCITY

```

75      GAM=ATAN(HI)
        VD=SQRT(2.*(EO-GE*H))
      *
      *
      *   CALCULATE SIN, COS AND POWERS OF COS GAMMA
      *
80      SG=SIN(GAM)
        CG=COS(GAM)
        CG2=CG**2
        CG3=CG*CG2
        CG4=CG*CG3
      *
      *
      *   DEFINE CURVATURE AND TIME DERIVATIVES OF CURVATURE, GAMMA,
      *   AND DESIRED VELOCITY
      *
90      XK=HII*CG3
        XK2=XK**2
        XK3=XK*XK2
        XK10=VD*(HII*CG+-3.*XK2*H)
        VD2=VD**2
        HI2=HI**2
        VD10=-GE*SG
        GAM10=XK*VD
        GAM20=XK10*VD+XK*VD10
        VD20=-GE*GAM10*CG
        XK20=(VD10*XK10)/VD - 10.*HI*XK*XK10*VD - 3.*VD2*XK3*
          (5.*HI2 + 1.)
      *
      *   DYNAMIC PRESSURE
      *
95      QB=RH0*VD2/2.
        QR10=RH0*VD*VD10
        QR20=RH0*(VD20*VD + VD10**2)
      *
      *
      *   UPDATE THRUST ESTIMATE TE AND DERIVATIVES (FIRST
      *   BACKWARD DIFFERENCE)

```

```

110      TE10=TE - TE10)/T
      TE=TR
      TE20=(TE10 - TE10P)/T
      TE10P=TE10

115      ESTIMATE ANGLE OF ATTACK AND DERIVATIVES

      SCLA=S*CLA
      CA=XMASS/(QB*SCLA + TE)
      CA2=CA**2
      QBST=QB10*SCLA + TE10
      CA10=-CA2*QBST/XMASS
      CA20=(-2.*CA*CA10*QBST - CA2*(QB20*SCLA + TE20))/XMASS
      VDG=VD2*XK + GE*CG
      VDG10=3.*VD*VD10*XK + VD2*XK10
      VDG20=3.*(VD10**2*XK + VD*VD20*XK) + 5.*VD*VD10*XK10 +
      VD2*XK20

125      ALE=CA*VDG
      ALE10=CA10*VDG + CA*VDG10
      ALE20=CA20*VDG + 2.*CA10*VDG + CA*VDG20

130      DETERMINATION OF ALPHA REFERENCE AND ELEVATOR REFERENCE

      Q3S=Q3*S
      CLAS=CLA + TE/QBS
      DCLO=(XMASS*VD2*XK + XMASS*GE*CG - TE*E)/QBS +
      CLQ*CBAR*(ALE10 + GAM10)/(2.*VD)
      DCMD=XIYY*(ALE20 + GAM20)/(Q3S*CBAR) -
      CMQ*CBAR*(ALE10 + GAM10)/(2.*VD)
      DENOM=CLAS*CMDE - CMA*CLDE
      ALR=(CMDE*DCLO - CLDE*DCMD)/DENOM
      DFR=(CLAS*DCMD - CMA*DCLO)/DENOM

```



```

145 * ALPHA DOT ESTIMATE UPDATED BY FIRST ORDER TAYLOR
    * EXPANSION
    *
    * ALR1D=ALE1D - CA*QBST*(ALR - ALE)/XMASS
150 *
    * PITCH RATE REFERENCE
    *
    * QR=ALR1D + GAM1D
    *
    * REFERENCE THRUST COMMAND
    *
    * CL=CLA*ALR + CLDE*DER + (CLQ*QR*CBAR)/(2.*VD)
    * CD=CDD + CL*2/PIARE
    * D=CD*QBS
    * TR=D/COS(ALR + E)
160 *
    * * * * *
    * TOTAL STATE REFERENCE VECTOR
    * ANGULAR QUANTITIES IN DEGREES
    * * * * *
    *
    * XD(1)=VD*COS(ALR)
    * XD(2)=VD*SIN(ALR)
    * XD(3)=QR*57.29573
    * XD(4)=(ALR + GAM)*57.29578
    * XD(5)=DER*57.29578
    * XD(6)=TR
    * XD(7)=H
165 *
    *
    *
170 *
    *
    *
175 * PRINT (8,100) R3,H,HI,4II,HII,XD(1),XD(2),XD(3),XD(4),XD(5),XD(6)
    *
    * IF(R3.GE.RI(NSP)) GO TO 90
    * PG=PG+XINC

```

```

180 GO TO 5
*
185 90 PRINT*
    PRINT*, "END OF DATA....."
    100 FORMAT(11(1X,E10.4))
    200 FORMAT(1I3)
    300 FORMAT (4(1X(E10.4)))
    400 FORMAT (5(1X(E10.4)))
    STOP
    END
1
*
*
*
*
*
5
*
*
*
*
*
10
*
*
*
*
*
*
*
*
*
*
15
DO 10 K=1,NSP
  IF(RG,GE,RI(K)) GO TO 10
  I = K
  50 TO 20
  10 CONTINUE
  I=NSP
  20 CONTINUE
  J = I - 1
  OR = RI(I) - RI(J)
  IF(OP.LE.0) GO TO 80
  OR2 = OR*OR
  OR3 = OR2*OR
25

```

```

3)  SIG = (RG - RI(J))/DR
      S2 = SIG*SIG
      S3 = S2*SIG
      DA = ALT(I) - ALT(J)
      *
      1 = ALT(J) + S2*(3. - 2.*SIG)*JA + ((SIG - 2.*S2 + S3)*SI(J) +
      *   (S3 - S2)*SI(I))*DR
      *
      HI = 6.*SIG*(1. - SIG)*DA/DR + (1. - 4.*SIG + 3.*S2)*SI(J) +
      *   (3.*S2 - 2.*S3)*SI(I)
      *
      HII = 6.*(1. - 2.*SIG)*DA/DR2 + ((6.*SIG - 4.)*SI(J) +
      *   (6.*SIG - 2.)*SI(I))/DR
      *
      -III = -12.*JA/DR3 + 6.*(SI(I) + SI(J))/DR2
      *
      RETURN
      80 PRINT*, "RANGE INCREMENT LESS THAN OR EQUAL TO ZERO!!"
      *
      RETURN
      END
4)
45

```


Appendix C

Table of

Discrete Feedback Gain Matrix Values*

Feedback Gain Matrix, \underline{K}
(Angular measurements in radian)

Sampling
Frequency

2 Hertz

.1881E-03	-.1339E-02	.5751E+00	.1192E+01	-.2469E+01	.1129E-06	.3044E-03
-.4170E+02	.4001E+01	-.3629E+04	-.1277E+05	.1138E+04	-.2912E-01	-.3768E+01

5 Hertz

.4056E-03	-.1430E-02	.1189E+01	.2498E+01	-.4614E+00	.2100E-06	.6713E-03
-.4240E+02	.3196E+01	-.3855E+04	-.1548E+05	.1039E+04	-.2939E-01	-.4566E+01

10 Hertz

.5622E-03	-.1394E-02	.1537E+01	.3389E+01	-.5740E+00	.2933E-06	.9242E-03
-.4279E+02	.2695E+01	-.4043E+04	-.1719E+05	.1019E+04	-.2954E-01	-.5071E+01

20 Hertz

.6696E-03	-.1351E-02	.1757E+01	.3992E+01	-.6434E+00	.3429E-06	.1096E-02
-.4301E+02	.2363E+01	-.4156E+04	-.1819E+05	.9924E+03	-.2963E-01	-.5366E+01

100 Hertz

.7743E-03	-.1300E-02	.1963E+01	.4575E+01	-.7071E+00	.3908E-06	.1262E-02
-.4320E+02	.2051E+01	-.4228E+04	-.1902E+05	.9556E+03	-.2970E-01	-.5615E+01

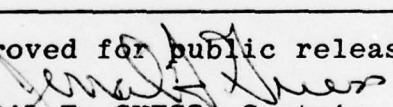
* Based on $q_1 = .0025$, $q_2 = 486.2$, $q_3 = 6.72E10$, $q_4 = .0001$, $r_1 = 1459$, $r_2 = 6.25E-08$

VITA

Ross Leon Simmons was born on 27 October 1942 in Salt Lake City, Utah. He was raised in Idaho Falls, Idaho, and attended Idaho Falls public schools. Upon graduation from Idaho Falls High School in June 1960, he enrolled at the University of Idaho, Moscow, Idaho. He completed the requirements for a Bachelor of Science in Electrical Engineering and was a Distinguished Graduate of the Air Force ROTC program receiving a regular commission in February 1965. In June of the same year he was assigned to pilot training. Upon completion of pilot training in June of 1966, he was selected for advanced training in the F-102 and F-101B fighter aircraft. In 1969 he retrained in the RF4C reconnaissance aircraft for a one year tour in Southeast Asia. Following the Southeast Asian tour, he completed a four year tour at RAF Alconbury, England. He was then stationed at Shaw Air Force Base, South Carolina, where he served in the capacity of instructor pilot, flight examiner, and flight commander for the 16th Tactical Reconnaissance Squadron. In 1976 Major Simmons was assigned to the Air Force Institute of Technology to obtain a Master of Science Degree in Electrical Engineering.

Unclassified

SECURITY CLASSIFICATION OF THIS PAGE (When Data Entered)

REPORT DOCUMENTATION PAGE		READ INSTRUCTIONS BEFORE COMPLETING FORM
1. REPORT NUMBER GE/EE/77-39	2. GOVT ACCESSION NO.	3. REPORT'S CATALOG NUMBER
4. TITLE (and Subtitle) THE TERRAIN FOLLOWING TASK FOR THE ADVANCED TACTICAL FIGHTER USING DISCRETE OPTIMAL CONTROL		5. TYPE OF REPORT & PERIOD COVERED MS Thesis
7. AUTHOR(s) Ross L. Simmons Major USAF		6. PERFORMING ORG. REPORT NUMBER
9. PERFORMING ORGANIZATION NAME AND ADDRESS Air Force Institute of Technology (AFIT-EN) Wright-Patterson AFB, Ohio 45433		8. CONTRACT OR GRANT NUMBER(s)
11. CONTROLLING OFFICE NAME AND ADDRESS Deputy for Development Planning (ASD-XRH) Directorate of Design Analysis Wright-Patterson AFB, Ohio 45433		10. PROGRAM ELEMENT, PROJECT, TASK AREA & WORK UNIT NUMBERS
14. MONITORING AGENCY NAME & ADDRESS (if different from Controlling Office)		12. REPORT DATE December 1977
		13. NUMBER OF PAGES 108
		15. SECURITY CLASS. (of this report) Unclassified
16. DISTRIBUTION STATEMENT (of this Report) Approved for public release; distribution unlimited.		15a. DECLASSIFICATION/DOWNGRADING SCHEDULE
17. DISTRIBUTION STATEMENT (of the abstract entered in Block 20, if different from Report)		
18. SUPPLEMENTARY NOTES Approved for public release; IAW AFR 190-17  JERRAL F. GUESS, Captain, USAF Director of Information		
19. KEY WORDS (Continue on reverse side if necessary and identify by block number) Digital Control Flight Control Terrain Following Discrete Optimal Control		
20. ABSTRACT (Continue on reverse side if necessary and identify by block number) Through the use of state space, continuous optimal control, and discrete optimal control, a digital flight control system was designed for the terrain following task. After formulating the aircraft linear perturbation model, the deterministic regulator problem was solved with a quadratic performance index to provide the desired continuous closed loop system. The system and performance index were then discretized to form a discrete deterministic regulator problem. This discrete regulator problem was then solved as		

Unclassified

SECURITY CLASSIFICATION OF THIS PAGE(When Data Entered)

a function of sample rate using eigenvector decomposition to determine a minimum acceptable rate for sampling. The effects of sample rate on the system were then examined. A sample rate of five hertz was shown to be high enough to adequately form the desired controls. A reference command generator based on constant energy path legs was developed to provide the required reference states and control inputs. The reference terrain following path was generated by an optimal cubic spline algorithm. The aircraft was shown to track the desired path in a highly acceptable manner through the use of a hybrid simulation. The design method utilized is recommended for consideration in designing the digital flight control system for other flight control tasks.

Unclassified

SECURITY CLASSIFICATION OF THIS PAGE(When Data Entered)